

1-1-2015

Assessing Viscoelastic Properties of Polydimethylsiloxane (PDMS) Using Loading and Unloading of the Macroscopic Compression Test

Mustafa Fincan

University of South Florida, mfincan@mail.usf.edu

Follow this and additional works at: <http://scholarcommons.usf.edu/etd>

 Part of the [Biomedical Engineering and Bioengineering Commons](#), and the [Materials Science and Engineering Commons](#)

Scholar Commons Citation

Fincan, Mustafa, "Assessing Viscoelastic Properties of Polydimethylsiloxane (PDMS) Using Loading and Unloading of the Macroscopic Compression Test" (2015). *Graduate Theses and Dissertations*.
<http://scholarcommons.usf.edu/etd/5480>

This Thesis is brought to you for free and open access by the Graduate School at Scholar Commons. It has been accepted for inclusion in Graduate Theses and Dissertations by an authorized administrator of Scholar Commons. For more information, please contact scholarcommons@usf.edu.

Assessing Viscoelastic Properties of Polydimethylsiloxane (PDMS) Using
Loading and Unloading of the Macroscopic Compression Test

by

Mustafa Fincan

A thesis submitted in partial fulfillment
of the requirements for the degree of
Master of Science in Materials Science and Engineering
Department of Chemical and Biomedical Engineering
College of Engineering
University of South Florida

Major Professor: Alex. A. Volinsky, Ph.D.
Nathan Gallant, Ph.D.
Manoj K. Ram, Ph.D.

Date of Approval:
April 8, 2015

Keywords: mechanical properties, soft material, viscoelasticity, elastic modulus, Zener model

Copyright © 2015, Mustafa Fincan

DEDICATION

I would like to dedicate my thesis to my parents who have always loved, supported, and encouraged me unconditionally. I am truly thankful for having you in my life. Thank you for all of your support along the years.

ACKNOWLEDGMENTS

First of all, I would like to express my special appreciation and thanks to my thesis advisor Dr. Alex A. Volinsky. I would also like to thank my committee members, Dr. Nathan D. Gallant and Dr. Manoj K. Ram, for your precious comments and suggestions. Many people, especially my best friends Necip Kayim, Metin Besalti, Mohammad Khawaja and also, Dr. Aytac Arikoglu, who is the professor at Istanbul Technical University, and Dr. Oguz Cimenler have made valuable comments and suggestions on this thesis, which gave me an inspiration to improve my work. Finally, I am grateful to everyone for their help directly and indirectly to complete my thesis.

TABLE OF CONTENTS

LIST OF TABLES	ii
LIST OF FIGURES	iii
ABSTRACT	vi
CHAPTER 1: INTRODUCTION TO MECHANICAL PROPERTIES OF POLYDIMETHYLSILOXANE	1
1.1 Mechanical Properties of Polymers	1
1.2 Modulus of Elasticity	2
1.3 Stress-Strain Behavior of Polymers	6
1.4 Viscoelasticity of Polymers	8
1.5 Structure, Properties and Uses of PDMS	13
CHAPTER 2: PDMS SYNTHESIS AND MECHANICAL CHARACTERIZATION	17
2.1 Synthesis and Characterization of PDMS	17
2.2 Mechanical Properties of PDMS under Linear Expansion	18
2.3 Mechanical Properties of PDMS under Non-Linear Expansion	23
2.4 Viscoelasticity Measurements Using Compression Testing	26
CHAPTER 3: PDMS MACROSCOPIC COMPRESSION TESTING	29
3.1 Samples Preparation and Equipment Setup	29
3.1.1 Samples Preparation	29
3.1.2 Compression Test Equipment Setup	31
3.2 PDMS Elastic Modulus Experimental Test Results	33
3.2.1 Macroscopic Test for Determining PDMS 5:1 Elastic Modulus	35
3.2.2 Macroscopic Test for Determining PDMS 10:1 Elastic Modulus	39
3.2.3 Macroscopic Test for Determining PDMS 20:1 Elastic Modulus	42
3.3 Conclusion of Macroscopic Compression Tests for PDMS Elastic Modulus	46
3.4 PDMS Viscoelasticity Experimental Test Results	51
3.4.1 The Kelvin–Voigt Model	51
3.4.1.1 Comparing the Kelvin–Voigt Model with Experimental Results	54
3.4.2 The Standard Linear Solid Model	60
CHAPTER 4: SUMMARY AND FUTURE WORK	64
REFERENCES	67

LIST OF TABLES

Table 1 Material constant values for different ratios of polymer and curing agent (PDMS-AB) using three non-linear models [27].....	24
Table 2 Macroscopic compression tests results for PDMS Poisson's ratio.....	32
Table 3 Macroscopic compression tests results for different samples of PDMS 5:1	36
Table 4 SPSS analyzed result of the elastic modulus of the PDMS 5:1 samples	39
Table 5 Macroscopic compression tests results for different samples of PDMS 10:1	40
Table 6 SPSS analyzed result of the elastic modulus of PDMS 10:1 samples	42
Table 7 Macroscopic compression tests results for different samples of PDMS 20:1	43
Table 8 SPSS analyzed result of the elastic modulus of PDMS 20:1 samples	46
Table 9 Elastic modulus of PDMS sample's experimental results	47
Table 10 Macroscopic compression tests results for different samples of PDMS 5:1	54
Table 11 Macroscopic compression tests results for different samples of PDMS 10:1	56
Table 12 Macroscopic compression tests results for different samples of PDMS 20:1	58
Table 13 PDMS 10:1 Elastic modulus on different petri dish	65
Table 14 Slopes of the spring compression test results	66

LIST OF FIGURES

Figure 1 Schematic of a typical stress-strain plot showing behavior of polymeric material at different stress levels.....	3
Figure 2 Von Mises yield condition for plastic flow in a cylindrical material, whose principal axis is parallel to the direction of increasing mean normal stress.	5
Figure 3 The Young's modulus values for a variety of hydrocarbons and polymeric materials as a function of the fraction of covalent bonds present in the materials	7
Figure 4 (a) Temperature dependence of E values for different types of polymers amorphous, cross-linked and crystalline; (b) E values and behavior at different temperature zones for polystyrene	8
Figure 5 Modeling viscoelastic behavior using a spring and a dashpot: (a) in series (Maxwell), or (b) parallel (Voigt), or (c) in combination (standard linear solid)	10
Figure 6 Stress relaxation for the Maxwell model; (a) with stress decaying to zero; (b) strain relaxation for the Voigt model, with strain saturating at ϵ_{∞} ; and (c) strain relaxation for the standard linear solid model, with strain saturating at ϵ_{∞}	11
Figure 7 Molecular structure of PDMS	14
Figure 8 (a) Changes in bulk storage modulus and (b) surface reduced elastic modulus of PDMS and another polymer, PVMS, as a function of time with UVO treatment.....	16
Figure 9 Viscosity of two commercially available PDMS samples: (a) as function of the shear rate and (b) the curing time	19
Figure 10 (a) Stress-strain curves for two types of PDMS; (b) resulting elastic moduli curves show an initial linear region.	20
Figure 11 (a) Casting mold for preparing test samples, (b) schematic diagram of a sample and (c) testing apparatus used for determining mechanical properties of two types of PDMS materials at strains	21

Figure 12 Strain-time relationship for a PDMS sample at constant temperature (23 °C) and constant stress value (3.125 N/mm ²)	22
Figure 13 Custom test apparatus for determining mechanical properties of PDMS with different amount of cross-linking.....	25
Figure 14 (a, b) Experimental and simulated curves showing load-deflection results and stress-relaxation results during punch test of PDMS samples; (c) Bulk storage and loss moduli at different loading frequencies under compression testing; and (d) Bulk stiffness values at different frequencies under cylindrical loading.....	27
Figure 15 PDMS base is mixed with curing agent and after it is stirred, air bubbles begin to appear	30
Figure 16 Cylindrical PDMS network samples for compression tests	31
Figure 17 PDMS compression test setup.....	32
Figure 18 PDMS compression setup for measuring elastic modulus	33
Figure 19 Comparison of preloading with no preloading on the same sample.	34
Figure 20 Distribution of different PDMS 5:1 samples' elastic modulus	38
Figure 21 SPSS analyzed result of the elastic modulus of the PDMS 5:1 samples.....	38
Figure 22 Distribution of different PDMS 10:1 samples' elastic modulus	41
Figure 23 SPSS analyzed result of the elastic modulus of PDMS 10:1 samples.....	41
Figure 24 Distribution of different PDMS 20:1 samples' elastic modulus	45
Figure 25 SPSS analyzed result of the elastic modulus of PDMS 20:1 samples.....	45
Figure 26 Distribution of different PDMS base/agent ratio samples elastic modulus.....	47
Figure 27 Distribution of diameter between 1 to 2 mm PDMS samples elastic modulus	48
Figure 28 Distribution of diameter between 2 to 3 mm PDMS samples elastic modulus	48
Figure 29 Distribution of diameter between 3 to 4 mm PDMS samples elastic modulus	49
Figure 30 Distribution of different PDMS crosslinking ratio samples elastic modulus	49

Figure 31 Schematic representation of the Kelvin–Voigt model.....	51
Figure 32 Applied stress and induced strain as function of time over a short period for the Kelvin-Voigt Model.	52
Figure 33 Comparison of PDMS 5:1 experimental results with the Kelvin - Voigt model for different samples.....	55
Figure 34 Comparison of PDMS 10:1 experimental results with the Kelvin - Voigt model for different samples.....	57
Figure 35 Comparison of PDMS 20:1 experimental results with the Kelvin - Voigt model for different samples.....	58
Figure 36 The standard linear solid model	60
Figure 37 Applied stress and induced strain as functions of time over a short period for the SLS model	61
Figure 38 Standard pen spring compression test results.....	65

ABSTRACT

Polydimethylsiloxane (PDMS) mechanical properties were measured using custom-built compression test device. PDMS elastic modulus can be varied with the elastomer base to the curing agent ratio, i.e. by changing the cross-linking density. PDMS samples with different crosslink density in terms of their elastic modulus were measured. In this project the PDMS samples with the base/curing agent ratio ranging from 5:1 to 20:1 were tested. The elastic modulus varied with the amount of the crosslinker, and ranged from 0.8 MPa to 4.44 MPa. The compression device was modified by adding digital displacement gauges to measure the lateral strain of the sample, which allowed obtaining the true stress-strain data. Since the unloading behavior was different than the loading behavior of the viscoelastic PDMS, it was utilized to assess viscoelastic properties of the polymer. The thesis describes a simple method for measuring mechanical properties of soft polymeric materials.

CHAPTER 1: INTRODUCTION TO MECHANICAL PROPERTIES OF POLYDIMETHYLSILOXANE

Polydimethylsiloxane (PDMS) belongs to an important group of polymeric compounds that have a wide range of commercial and industrial applications, and are also known as silicones. Hybrid-glass and PDMS-based polymers are used in different areas ranging from optoelectronics, medicine and cosmetics, surfactants and industrial cleaning agents, soft lithography, encapsulating biomaterials and others. As of recently, the material is being actively researched as a substrate carrier for long term neural implants because of the unusual mechanical and electrical properties that it possesses [1, 2]. Many of these properties are common to the polymers family, while some interesting properties are unique to the PDMS group. In the next section properties of polymers in general, in particular, their mechanical properties, and their measurements, are discussed.

1.1 Mechanical Properties of Polymers

Polymers are essentially large molecules, either natural or synthetic, created through carbon bonds and repeated units that are either organic or inorganic in nature [3, 4]. Polymers are typically synthesized using intermolecular reactions between molecules with at least two functional groups. The functional groups, such as a strong nucleophile and an alkyl halide react with each other to give rise to a product, which then reacts with a third functional group. The reaction products in turn react with a fourth functional group, and so on [2-4]. Synthetic polymers are usually synthesized from smaller molecules called monomers, which are added

successively using ester and amide bonds. Properties of polymers can be extensively customized by choosing suitable monomers as well as bonding agents.

The elasto-mechanical properties of polymers are often intermediate between corresponding properties of solids and liquids. The reason is that in the solid state polymer molecules either form random groups (amorphous state) or regular arrays (crystalline state) that are closely packed and do not have large intermolecular gaps or voids. On the other hand, a polymer that is in a solution has each molecule surrounded by a large number of solvent molecules, thereby giving properties that are more similar to liquids than solids. Most polymers, however, have a high degree of polymerization, or a large number of repeating groups, so that they have their distinct properties that are common to the polymer family. The mechanical properties of polymers are also influenced by the architecture of the molecules, whether they consist of linear chains, cross-chains or cross-linked chains [2, 4]. In particular, extensively cross-linked polymers might have one single super-molecule in a container: PDMS is an example of such a polymer.

1.2 Modulus of Elasticity

It would be worthwhile to have a general overview of the elastic modulus, viscoelasticity and other mechanical properties of materials before discussing the corresponding properties of PDMS. One of the principal characteristics of any material is how it behaves when it is subjected to an externally applied force. Under such conditions the material deforms either elastically or plastically. The deformation under elastic conditions is reversible in nature and it is linear for many materials. Linear deformation usually obeys a relation that is called the Hooke's law, which states that the applied stress is proportional to the strain. The constant of proportionality is called the Young's modulus of the modulus. The relation is:

$$\frac{F}{A} = E \frac{\Delta L}{L} \quad \text{or} \quad \sigma = E\varepsilon \quad (1)$$

where σ denotes applied stress, ε represents resulting strain and the proportionality constant E is the Young's modulus of the material, which can also be defined as the ratio of stress to strain. As can be observed, stress is expressed as the ratio of applied force (F) to the cross-sectional area (A) over which it acts, while strain is defined as the deformation over a unit length [2, 5, 6].

From equation (1) it can also be observed that Young's modulus is directly proportional to the stress and is inversely proportional to the strain. The stress and strain in equation (1) may be either tensile or compressive.

A standard test of tensile properties of a material is performed by slowly increasing stress on a specimen from zero to the value at which the specimen fractures. The strain at each incremental stress value is measured and a stress-strain plot is obtained, as shown in Figure 1.

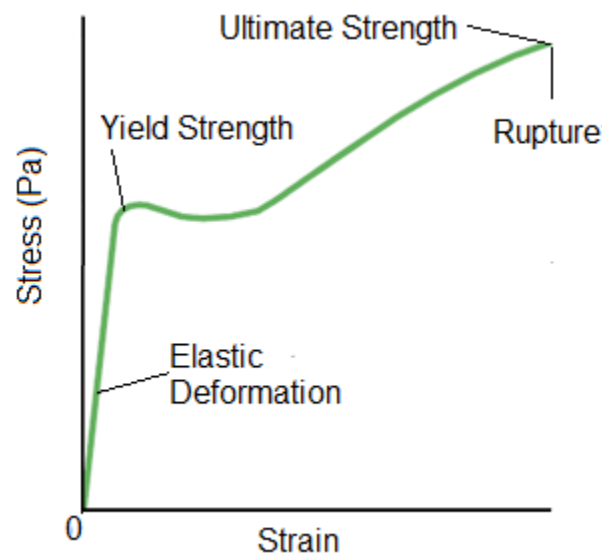


Figure 1 Schematic of a typical stress-strain plot showing behavior of polymeric material at different stress levels. Adapted from [6].

It can be observed from Figure 1 that the stress-strain graph is a straight line, or linear, over a substantial portion of the total deformation curve. The point at which linearity breaks down and permanent deformation begins is called the yield strength of the material, while the point at which the specimen finally ruptures is called its ultimate strength [2, 6].

Materials under an applied force deform through three principal mechanisms: by transmitting the applied force directly to intermolecular bonds and interatomic interactions; or by undergoing substantial shape changes; or by deforming either semi-permanently or permanently. The first type of deformation is typical of rigid and crystalline substances, such as bones, celluloses and most solids. These are also called Hookean materials because their response is mainly governed by the linear part of the stress-strain graph in Figure 1. Crystalline polymers also fall in this category. The strain resulting from the applied force for these materials is often called the Cauchy strain, ϵ_c , and the mode of deformation is said to be elastic. There are other modes of deformation, such as shear and bulk deformation. Shear modulus G for an isotropic material is expressed in terms of the Young's modulus, E , and the Poisson's ratio, ν , as follows:

$$G = \frac{E}{2(1+\nu)} \quad (2)$$

The second type of deformation, in which materials undergo substantial shape change due to applied force, is typical of non-crystalline polymers and soft biological materials. These so-called non-Hookean materials experience a different type of strain, known as the true-strain, the Hencky strain, which is expressed as:

$$\epsilon_H = \ln\left(\frac{L_0 + \Delta L}{L_0}\right) = \ln(1 + \epsilon_C) \quad (3)$$

An important feature of the Hencky strain is that it is an instantaneous measure, so that the material does not retain a memory of its strain history.

The third type of deformation, which is either permanent or semi-permanent, is exhibited by amorphous polymers and many other materials at high stress levels. Polymeric materials under these conditions may undergo plastic deformation, also called plasticity or ductility, and then experience ductile failure with yield. The yield occurs through plastic deformation and is often accompanied by an abrupt reduction in cross-section (necking). The molecules reorient themselves in the necked region along preferred orientations, resulting in a sample that is actually harder than the initial amorphous material, a phenomenon known as strain hardening. Plasticity in materials is probed using tension along one axis. The ductile specimen undergoes a sudden transition from a linear elastic loading behavior to plastic flow when the stress reaches the yield strength. In case of the stresses along the three axes, σ_1 , σ_2 , σ_3 , plastic flow starts when the equivalent stress $\bar{\sigma}$ reaches the yield strength and this generalized condition is called the Von Mises yield condition. This is shown in Figure 2.

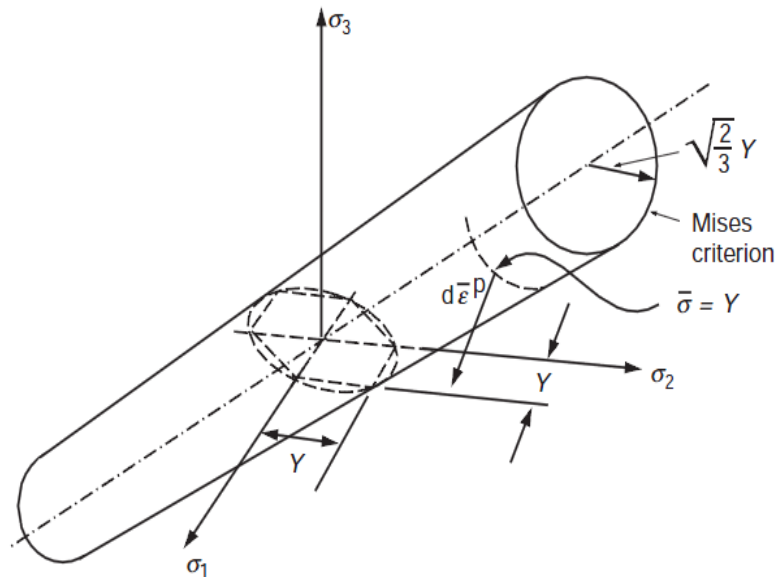


Figure 2 Von Mises yield condition for plastic flow in a cylindrical material, whose principal axis is parallel to the direction of increasing mean normal stress. Adapted from [6].

1.3 Stress-Strain Behavior of Polymers

Many polymers exhibit stress-strain behavior that is somewhat similar to solids, but an important characteristic of such materials is that their mechanical properties vary with the rate of developed strain, as well as temperature. As discussed in the previous section, deformation can occur through brittle, plastic or highly elastic routes. The values of the Young's modulus and tensile strength for polymers are much lower than metals, while some polymers can elongate by as much as 1,000% of their original length. In addition, the mechanical properties of many polymers change significantly with temperature, from brittle to highly elastic behavior as temperature increases. An important characteristic of plastic flow regime in polymers is the principle of maximum plastic dissipation. According to this principle, the state of stress actually present in a sample for a given plastic strain increase results in an increment of work that is either equal to or greater than the work done by the plastic strain increase with any other state of stress, within or on the yield surface [2, 7]. This principle gives rise to the associated flow rule, which states that each individual plastic strain increase is proportional to the component of an outward stress vector acting normal to the yield surface.

The Young's modulus of polymers is highly dependent on their chemistry as well as the temperature. The value of E for these materials increases as covalent bonds aligned to the loading axis increases, with cross-linked polymers having the Young's modulus values between 50 to 100 GPa [7, 8]. This is shown in Figure 3.

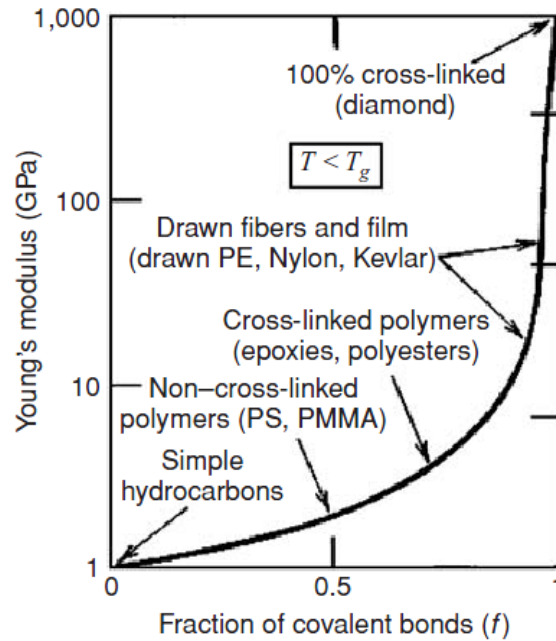


Figure 3 The Young's modulus values for a variety of hydrocarbons and polymeric materials as a function of the fraction of covalent bonds present in the materials. Adapted from [8].

As the applied temperature is increased, the Young's modulus value for different types of polymers decreases. Amorphous polymers have a random chain arrangement below the glass transition temperature, T_g ; therefore, their E values decrease slowly as temperature is increased to T_g . At the glass transition temperature their molecules can rotate favorably around the single bonds, causing a sharp decrease in the E values. Thereafter these materials exhibit a large amount of plastic or rubbery deformation, until the melting point, T_m is reached. On the other hand polymers with more cross-linking undergo greater chain rotation as temperature is increased, thereby having a more stable E value in the region between T_g and T_m . A cross-linked polymer, such as PDMS, exhibits greater impact resistance in this region [7-10]. This is shown in Figure 4, which compares the dependence of E values on temperature for different types of polymers and for the specific compound polystyrene [8].

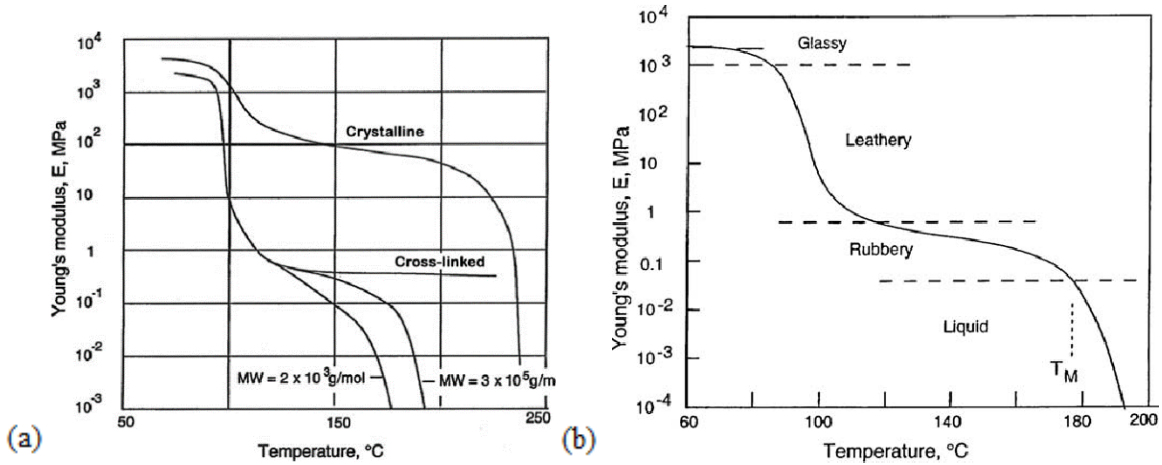


Figure 4 (a) Temperature dependence of E values for different types of polymers – amorphous, cross-linked and crystalline; (b) E values and behavior at different temperature zones for polystyrene. Adapted from [8].

1.4 Viscoelasticity of Polymers

Polymers deform elastically at lower temperatures and like a viscous liquid at higher temperatures, but at intermediate temperatures they exhibit a behavior that is similar to a rubbery solid, known as viscoelastic deformation. This is a very important property for polymers and most biological materials because they possess cross-linked crystalline structures that are more or less viscoelastic in nature [9]. Viscoelasticity is defined as the response of a fluid or solid, which is a combination of viscous and elastic behavior, as determined by the rate of deformation relative to the relaxation time of the material. It can be both linear and non-linear, but linear viscosity is an especially useful study area for many engineering applications of polymers and composite substances [9, 10]. PDMS is a semi-crystalline thermoplastic, implying that it can be repeatedly softened by the application of heat and solidified by removal of heat. The storage (E') and loss modulus (E'') in viscoelastic materials measure the stored energy, representing the elastic portion, and the energy dissipated as heat, representing the viscous portion [11, 12].

$$E' = \frac{\sigma_0}{\varepsilon_0} \cos\delta \quad (4)$$

$$E'' = \frac{\sigma_0}{\varepsilon_0} \sin\delta \quad (5)$$

σ and ε denote dynamic stress and strain, and they defined as follows:

$$\sigma = \sigma_0 \sin(\omega t + \delta) \quad (6)$$

$$\varepsilon = \varepsilon_0 \sin(\omega t) \quad (7)$$

δ is the phase lag between the stress and the strain, t is time. Time is usually described as a rate specified by the frequency: $\omega = 2\pi f$ [11, 12].

Viscosity, η , of a Newtonian fluid is mathematically expressed as the ratio of shearing stress to the strain rate:

$$\eta = \frac{F/A}{d\varepsilon/dt} \quad (8)$$

The shear modulus, G , defined in equation (2) earlier, can also be expressed in a similar manner:

$$G = \frac{\tau}{\gamma} = \frac{F/A}{\Delta x/A} \quad (9)$$

On the other hand, viscoelastic behavior implies that polymeric fluids can behave like an elastic solid under some conditions and like a viscous fluid under other conditions. The primary difference between elastic and viscoelastic deformation is that in case of the latter there is a time-dependent deformation of the material, at least part of which is recoverable subsequently.

Viscoelastic behavior can be modeled using a spring and a dashpot (or a motion damper) in series (also called the Maxwell model), or parallel (also called the Voigt model), or a combination of the two, as shown in Figure 5.

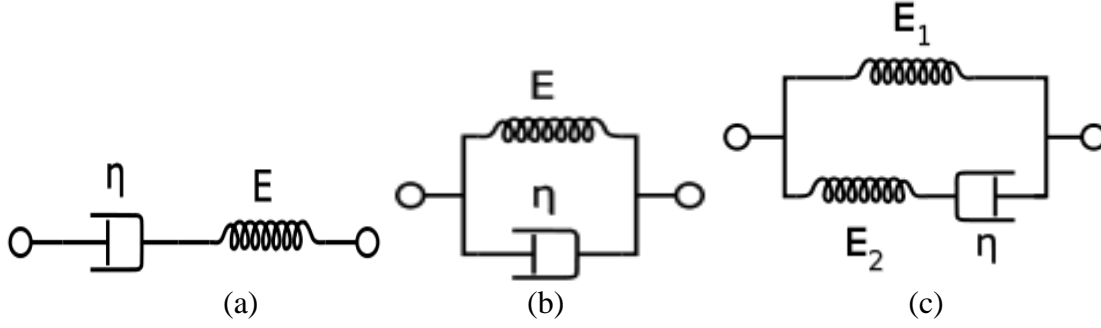


Figure 5 Modeling viscoelastic behavior using a spring and a dashpot: (a) in series (Maxwell), or (b) parallel (Voigt), or (c) in combination (standard linear solid). Released into public domain by Pekaje, 2007 [13].

The change in length of an elastic (Hookean) spring having a spring constant E under a constant force F is given by

$$\varepsilon_s = F/E \quad (10)$$

while the change in length of a viscous (Newtonian) dashpot, having a dashpot constant η under a constant force F , is given by

$$\frac{d\varepsilon_D}{dt} = F/\eta \quad (11)$$

If there is a sudden application of a constant force F at time $t = 0$, the immediate response of the spring is given by equation (6), but the time-dependent response of the dashpot is given by $\varepsilon_D t = F_D t/\eta$. The overall response for a series arrangement (Maxwell model) is given by

$$\varepsilon = \varepsilon_s + \varepsilon_D = F/E + Ft/\eta \quad (12)$$

In this case, the strain rate is constant and the viscous strain is not recovered if the force is removed. In case of a parallel arrangement (Voigt model), the overall response is given by

$$\varepsilon = \varepsilon_s = \varepsilon_d = \varepsilon_\infty [1 - \exp(-t/\tau)] \quad (13)$$

where ε_∞ represents elongation of the spring at infinite time when it carries all the applied force, and τ represents a relaxation time defined as the ratio of the dashpot and the spring constants, so

that $\tau = \eta/E$. In case of a series and parallel combination, the forces applied are $F = F_1 = F_2 + F_d$ (force F is applied at $t = 0$), while the elongations are $\varepsilon_v = \varepsilon_2$ and $\varepsilon = \varepsilon_1 = \varepsilon_2$. The overall response is given by

$$\varepsilon = \varepsilon_\infty - (\varepsilon_\infty - \varepsilon_0)\exp(-t/\tau_s) \quad (14)$$

where ε_0 represents the initial or unrelaxed expansion of the spring and τ_s is defined as the relaxation time required for strain relaxation, so that $\tau_s = \eta/E_2$. The stress and strain relaxations corresponding to the three models are shown in Figure 6.

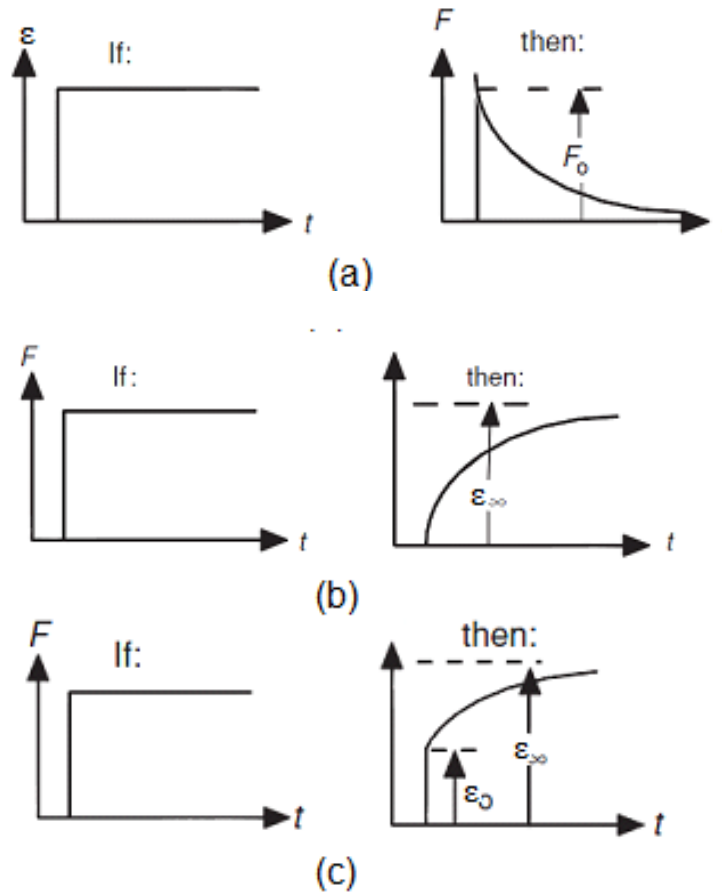


Figure 6 Stress relaxation for the Maxwell model; (a) with stress decaying to zero; (b) strain relaxation for the Voigt model, with strain saturating at ε_∞ ; and (c) strain relaxation for the standard linear solid model, with strain saturating at ε_∞ . Adapted from [8].

It has been found that the elongation of polymers under constant applied force is most closely simulated by the combined model. Sometimes better results are also obtained by using a number of Maxwell and Voigt models, but not combining them into a single simple-parallel configuration, so that different number of models yield different time characteristics that are similar to the actual polymer behavior [8]. One such combination is called the “standard linear solid”, which essentially consists of an elastic spring placed in parallel to the Maxwell model. The advantage of this configuration is that it retains a rubbery stiffness after the dashpot in the Maxwell model has expanded and the stresses have relaxed, thus providing a close simulation of the behavior of an actual polymer [8-10]. The time-dependent stress-strain relationship corresponding to both creep and stress relaxation is given by

$$\sigma + \frac{\eta}{E_m} \frac{\partial \sigma}{\partial t} = E_v \varepsilon(t) + \frac{\eta(E_v + E_m)}{E_m} \frac{d\varepsilon}{dt} \quad (15)$$

The standard linear solid configuration can effectively model both the stress relaxation exhibited by a viscoelastic polymer and its creep behavior that results in permanent deformation under a constant stress over time [15]. Another combination model often used to study creep is the four parameter Burger’s model, in which a Voigt model is used in series with a spring and a dashpot [17]. The strain ε is expressed as a sum of the elastic strain, viscous (creep) and viscoelastic strains:

$$\varepsilon = \varepsilon_{\text{elastic}} + \varepsilon_{\text{viscous}} + \varepsilon_{\text{viscoelastic}} \quad (16)$$

The strain is calculated in terms of properties of springs and dashpots as follows:

$$\varepsilon = \frac{\sigma}{E_m} + \frac{\sigma t}{\eta_m} + \frac{\sigma}{E_v} (1 - e^{-t/\tau}) \quad (17)$$

where E_m and E_v represent the modulus of elasticity of the two springs and η_v represents the viscosity of the dashpot.

1.5 Structure, Properties and Uses of PDMS

Polydimethylsiloxane (PDMS) is a highly cross-linked semi-crystalline thermoplastic material. It is unique among polymers because it has a silicon-oxygen backbone instead of a carbon backbone, which is more commonly found. Because of this it has a lower glass transition temperature of $-125\text{ }^{\circ}\text{C}$, which in turn makes it less temperature sensitive than other rubber like polymers. It is used in membrane oxygenators because of its high oxygen permeability. It is highly flexible and biologically stable, which is why it is often used in sensitive medical equipment, such as catheter and drainage tubing, and in insulation for pacemakers. It is also used in prostheses, such as finger joints, blood vessels, heart valves and other implants [16]. Commercially available PDMS is known by various names, including Siloxanes, Silicone fluids, Dimethicone and E900. It is manufactured commercially by carrying out a reaction between elementary silicon and methyl chloride, CH_3Cl . The reaction yields dimethyl dichlorosilane, $\text{Si}(\text{CH}_3)_2\text{Cl}_2$, which is distilled and hydrolyzed to form linear siloxanes and is further polymerized. Smaller molecular weight siloxanes are removed by thermal treatment, or through solvent extraction [17].

Physically, it is a clear odorless liquid with very low vapor pressure with properties that are marginally dependent on its degree of polymerization (which in turn determines its viscosity). It has a chemical formula of $(\text{C}_2\text{H}_6\text{OSi})_n$ with n representing the number of repeated units, and its molecular structure is shown in Figure 7.

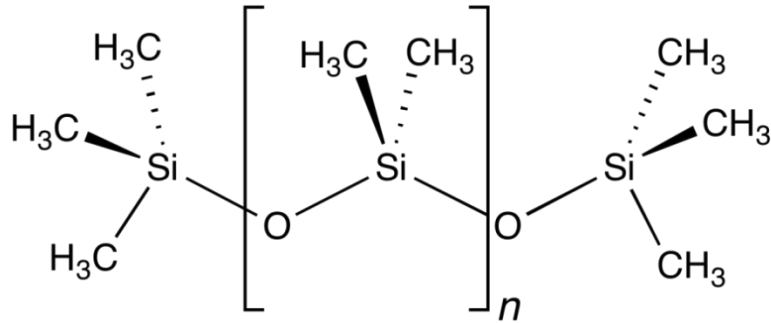


Figure 7 Molecular structure of PDMS [18].

It can be observed in Figure 7 that PDMS has an inorganic backbone with organic groups as pendants, so it is classified as a “semi-inorganic” or “organic-inorganic” polymer. PDMS and silica composites have a fairly high impact strength, which determines the ability of a material to withstand a sudden fracturing force. The use of standard impact tests, such as the Charpy pendulum and the falling weight impact tests on PDMS composites have led to the conclusion that impact strength increases as the percentage of PDMS in a composite increases. This is because the siloxane component behaves as an elastomer due to its glass transition temperature being much lower than room temperature. It can absorb large quantities of energy during an impact test, resulting in delayed development of cracks and fractures [2, 19]. Although bulk PDMS has relatively low thermal conductivity of 0.15 W/mK, it has recently been noticed that single or double polyethylene chains that constitute amorphous or crystalline PDMS display higher conductivity values of 7 W/mK. This finding may lead to wider use of the material as a thermal grease [20].

The surface properties of PDMS and composite polymers have been of particular interest for quite some time due to the wide applications areas of these materials. Many of these applications are due to useful characteristics of PDMS, such as low intermolecular forces between and compact sizes of the pendant methyl groups, high flexibility and bond energy of the

siloxane backbone, and the partial ionic nature of the siloxane bond [21]. PDMS in the solid state has a hydrophobic surface, so a solid sample of the material does not swell in the presence of water or alcohol-based solvents. However, some organic solvents can diffuse into the samples and cause swelling. On the other hand, treatment of the surface by air or argon plasma adds silanol groups and thereby renders the sample surface hydrophilic. This allows PDMS to be used in a number of microfluidic applications, such as forming patterned nanoparticle arrays and optoelectronic packages. Another popular method of increasing surface hydrophilicity is ultra-violet ozone (UVO) treatment, in which short wavelength UV rays and atomic oxygen are used to form volatile organic molecules that desorb from the sample surface [21, 22]. Longer duration UVO treatment (5-10 minutes) is used to deposit hard silica-like layers of 5 nm approximate thickness on the surface of the polymer. It also leads to changes in mechanical properties of PDMS due to the densification of cross-linked silicone elastomer networks at or near the surface. Dynamic mechanical thermal analysis (DMTA) and nanoindentation techniques have been used to determine changes in elastic modulus as a function of UVO treatment time of PDMS samples. It has been found that the storage modulus remains constant but the elastic modulus increases by a small amount as treatment time is increased [21]. This is shown in Figure 8.

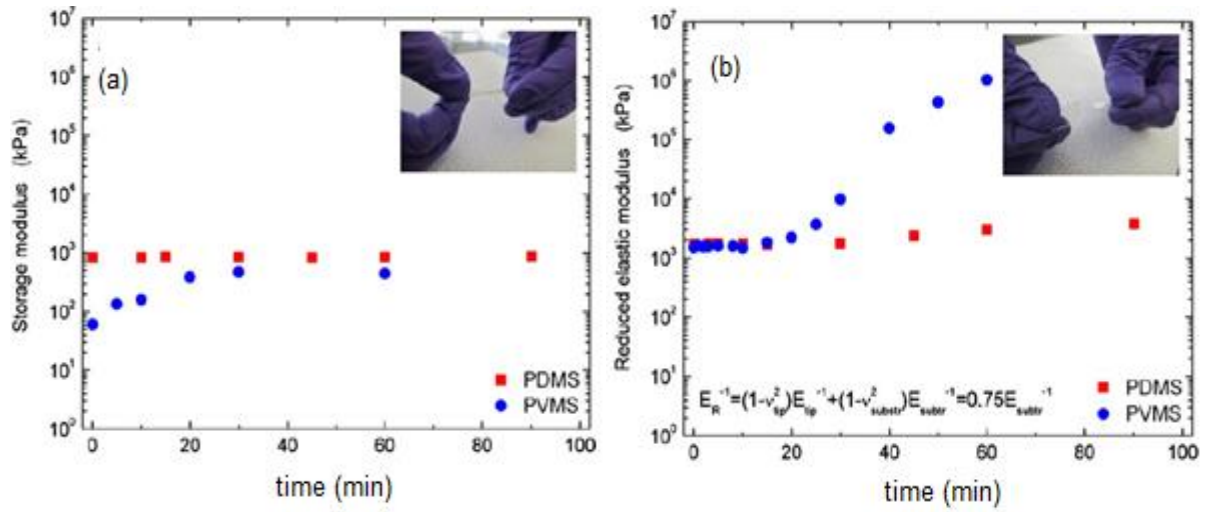


Figure 8 (a) Changes in bulk storage modulus and (b) surface reduced elastic modulus of PDMS and another polymer, PVMS, as a function of time with UVO treatment. Red squares represent PDMS while blue circles represent PVMS (poly vinyl methyl siloxane). Adapted from [21].

CHAPTER 2: PDMS SYNTHESIS AND MECHANICAL CHARACTERIZATION

The synthesis routes and properties of PDMS and related composite polymer materials have been researched by investigators for quite some time, and a wide variety of characterization techniques have been employed so far.

2.1 Synthesis and Characterization of PDMS

The possibility of using polyurethanes based on PDMS and mono methoxypolyethylene glycol (MPEG) as polymeric biomaterial for coatings was investigated by Park et al. [23]. The authors used commercially available PDMS and ethylene glycol as base materials to prepare MPEG grafted polyurethane (PU) sheets utilizing a two-step condensation reaction. The resulting polymers were characterized using attenuated total reflectance infrared spectroscopy, proton nuclear magnetic resonance (H-NMR), gel permeation chromatography, and other techniques. Results indicated that the PDMS phase grafted onto the PU substrate to create soft and hard segments of polymers, but there was a good degree of phase separation, since hydrogen bonding between carbonyl and N-H groups in PU occurred only in the hard segment [22, 23]. The authors also observed that the surface molecules were oriented in such a manner that interfacial energy between the polymer and air, or water, was minimized. This resulted in the commonly observed hydrophobic surface, especially in the absence of surface impurities and rough surfaces. Because of the process, the advancing effect of PDMS-based polymers were observed to be high [23].

2.2 Mechanical Properties of PDMS under Linear Expansion

PDMS was used as an impact modifier for epoxy resins and the resultant mechanical properties of the polymer networks were investigated by Hanoosh & Abdelrazaq [24]. The reason they chose epoxy resins as the substrate was that this group of toughened thermoset resins are particularly useful in the manufacture of composite fiber reinforced plastic materials. The resins is, however, brittle in nature and require modifiers, such as carboxyl terminated polybutadiene co-acrylonitrile or PDMS. The elastomer was prepared by cross-linking hydroxyl terminated polydimethylsiloxane with tetraethyl orthosilicate with tin (II) 2-ethylhexanoate acting as one of the catalysts. Samples were characterized using Fourier transform infrared spectroscopy and H-NMR, while mechanical properties were assessed using tensile, flexural and compressive testing as well as dynamic mechanical analysis [24]. The authors observed that increasing the ratio of PDMS in the epoxy resin led to increased toughness of the final product, with elongation increasing from 22% to 39% as PDMS content increased from 0% to 20%. On the other hand, values of the ultimate compression strength and ultimate tensile strength both decreased as PDMS content increased. In addition, storage and loss moduli were both found to decrease, both as a function of temperature and as a function of PDMS content [2, 24]. The authors found that all the epoxy resin specimens transitioned from stiff and hard solids to pliable polymers as temperature increased, signaling decreases in their storage moduli. Based on their results the authors concluded that the optimum toughness level of the composite occurred at 5% PDMS content.

Mechanical and rheological properties of PDMS materials for application as micro electromechanical systems (MEMS) packages was also investigated by Schneider et al. [25]. PDMS is used as a cast to embed electronic components and increase their operational lifetime,

so the authors were interested in determining these properties with a view to designing improved microcircuits. They used a cone plate viscometer to measure shear-dependent viscosity of two commercially available PDMS samples, Sylgard 184 and RTV 615 [25]. The instrument used by them measured viscosity as functions of torque and cone positions, with the applied rotational frequency determining the cone's moment of inertia. Both silicone elastomers showed very similar viscosity properties of viscosities at shear rates between 0.01 s^{-1} and 30 s^{-1} at room temperature. It was also observed that the samples behaved as Newtonian fluids, with viscosity values being independent of the shear rate. Hardening of the materials was investigated by applying a uniform shear rate of 30 s^{-1} and measuring the viscosity over time. The authors found that Sylgard 184 underwent a faster hardening process at $60 \text{ }^\circ\text{C}$ compared to RTV 615 – the viscosity of the former increased by 8% and of the latter by 5.5% during a 15 minutes observation interval. These results are shown in Figure 9.

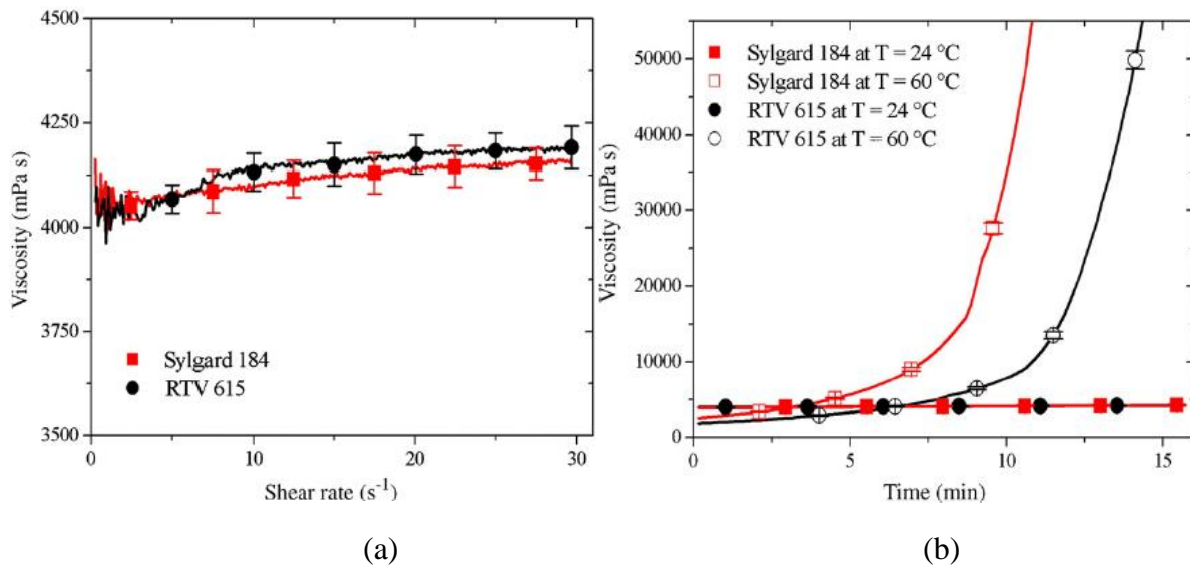


Figure 9 Viscosity of two commercially available PDMS samples: (a) as function of the shear rate and (b) the curing time. The graph (a) shows an irregular curve because measurements were performed continuously. Adapted from [25].

The authors also determined the constant elastic moduli of the two materials over a large strain range, up to 115%. The tests were performed with rectangular samples with a high length to width ratio of 20 in order to reduce the effects of clamping in the tensile testing apparatus. A constant strain rate of 0.1 mm/sec was used to pull one end of the sample with the resulting force was recorded. The derivative of the resulting stress-strain curve was used to calculate the modulus of elasticity, E. For both tested elastomers the authors obtained curves that were linear up to 45% strain, yielding E values of 1.76 MPa for Sylgard 184 and 1.54 MPa for RTV 615 [25]. Beyond the linear region the E values of both materials increased non-linearly up to 92-97% strain and thereafter the E values decreased. The results, however, had high standard deviation because of errors introduced by the clamping mechanism of the apparatus. The stress-strain diagrams and E values for both materials are shown in Figure 10.

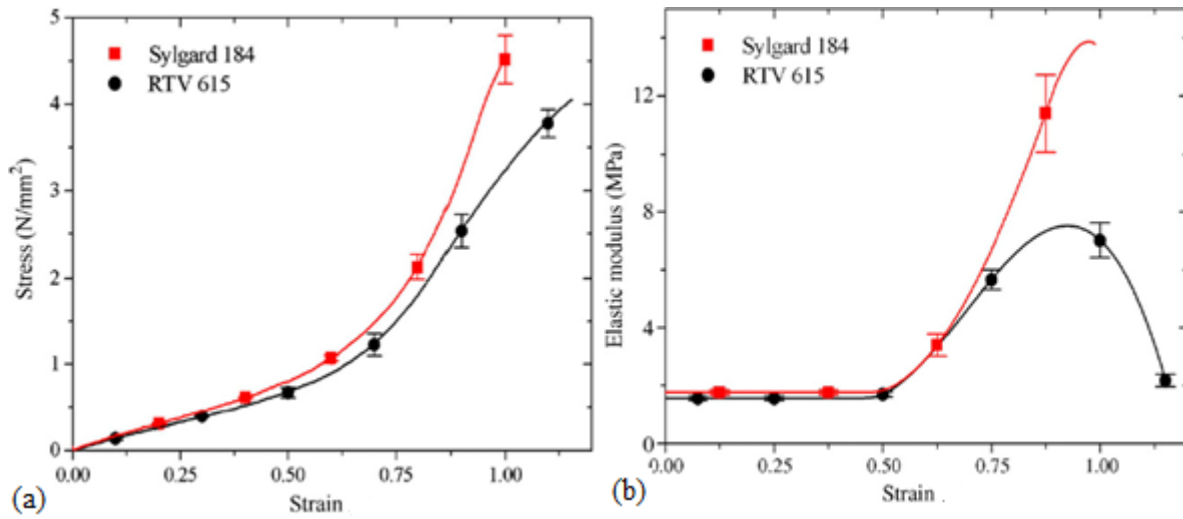


Figure 10 (a) Stress-strain curves for two types of PDMS; (b) resulting elastic moduli curves show an initial linear region. This is followed by increasing and then decreasing E value regions. Adapted from [25].

While the above results were obtained for high strain values, the mechanical properties of the elastomers were also obtained for lower strain values up to 45%. Tensile tests were carried out to determine tear strength, tensile strength, strain at break and stress values using test bars prepared in accordance with the DIN 53504 standard [26]. The mold used to prepare the samples and the testing apparatus are shown in Figure 11.

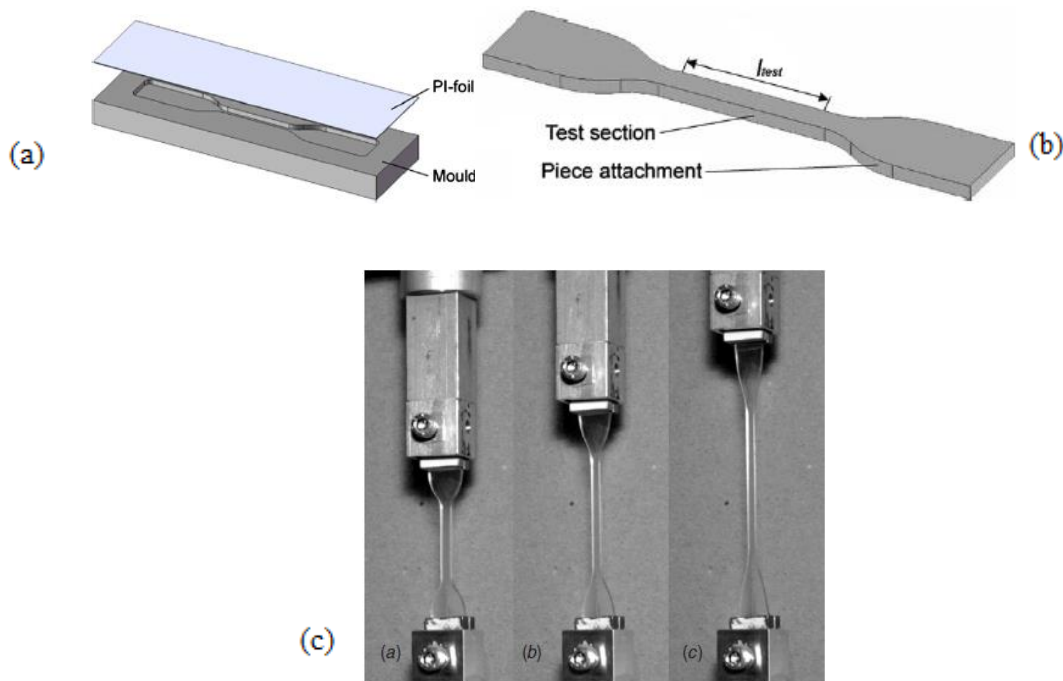


Figure 11 (a) Casting mold for preparing test samples, (b) schematic diagram of a sample and (c) testing apparatus used for determining mechanical properties of two types of PDMS materials at strains. Adapted from [26].

The authors found that the addition of a thinner (which reduced the viscosity of the sample bars) at different concentrations significantly affected the sample mechanical properties. Elastic moduli of all samples tested decreased as thinner concentration was increased from 0% to 10%, while the elastic modulus of a sample at a given thinner concentration was found to be

linearly dependent on temperature. The authors found that this dependence closely followed the relation

$$E = \frac{2}{3}kT\rho_k \quad (18)$$

where k denotes the Boltzmann's constant, T denotes absolute temperature and ρ_k denotes the degree of cross-linking present in the PDMS sample. In addition to establishing temperature dependence, the authors also found that the viscoelastic properties of the elastomers were dependent on the strain rate. They measured a 2% increase in elastic modulus for Sylgard 184 when the applied strain rate was within 0.0025/s to 0.1/s range. The creep properties were measured using the Burger's model described by equations (12) and (13). It was found that creep increased as thinner content was increased, with the strain increasing due to increasing viscous and viscoelastic creep parameters. However, the authors were not able to find a systematic relation for variations in the time constant of equation (13). The strain time diagram illustrating increasing strain values for higher thinner content is shown in Figure 12.

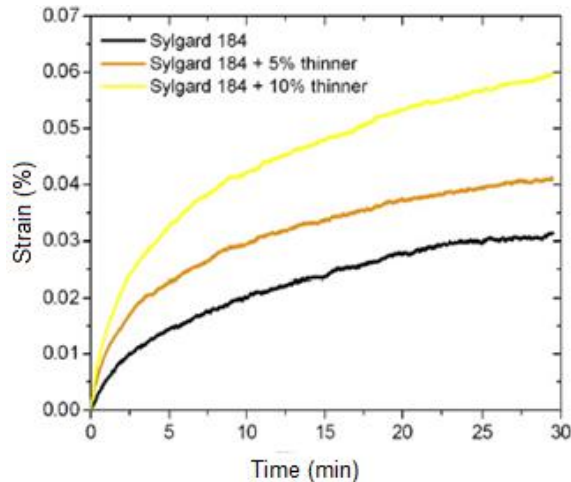


Figure 12 Strain-time relationship for a PDMS sample at constant temperature (23 °C) and constant stress value (3.125 N/mm²). Adapted from [26].

2.3 Mechanical Properties of PDMS under Non-Linear Expansion

The papers reviewed so far concentrated mainly on the mechanical properties of different types of PDMS in their linear extension regions. Different mechanical properties of PDMS in the non-linear region were investigated by Kim, Kim, & Jeong [27]. The purpose of their investigations was that while PDMS materials are used in a wide variety of devices, including optoelectronic packaging, microfluidic devices and critical medical equipment, there are almost no literature reports on the behavior of these materials under nonlinear conditions that involve stress softening and residual strains [27]. The authors also considered the fact, illustrated in the two previous papers reviewed in this section, which mechanical properties of PDMS depend on the ratio of the pure polymer and thinners, or the curing agents used. This dependency was earlier explained by Unger et al. as being a result of structural or covalent bonding that occurs between more flexible vinyl PDMS and more rigid Silicon-Hydride (Si-H) based PDMS sections [27, 28].

Kim et al. performed one-time failure tension tests, as well as cyclic fixed strain tests and used three non-linear models (Neo-Hookean, Mooney-Rivlin and Ogden) to simulate mechanical properties from their obtained stress-strain curves. The tests were carried out on bar shaped samples prepared from three variants of Sylgard 184. They found that the use of 5% curing agent (designated as PDMS-05) did not change stress values at 50% cyclic strain levels, but introduced hysteresis of the material at 100% cyclic strain. In addition, the stress was found to decrease after several loading-unloading cycles were carried out. The magnitude of decrease was found to be highest after the 1st and 2nd cycles, after which it became less – the magnitude was also found to be higher in the higher strain region. Somewhat similar results were obtained at 10% and 15% concentration levels (designated as PDMS-10 and PDMS-15, respectively). However,

increasing curing agent levels resulted in increased yield stress at low strain levels. From these observations the authors concluded that both hysteresis and yield stress values can be controlled by increasing polymer content or decreasing the curing agent content. Evaluating the three non-linear models, the authors found that the 2nd order Ogden model came closest to predicting the non-linear portion of the stress-strain curves. This model was also found to simulate the increase in bulk modulus of the samples as curing agent concentration was increased [27]. Material properties obtained by the authors for different ratios of polymer and curing agent (designated as PDMS-AB) are shown in Table 1.

Table 1 Material constant values for different ratios of polymer and curing agent (PDMS-AB) using three non-linear models. Adapted from [27].

Material Model	Material Constants	PDMS-AB (Base Polymer: Curing Agent)		
		5%	10%	15%
Neo-Hookean	C_{10} (MPa)	0.209	0.0705	0.093
Mooney-Rivlin	C_{10} (MPa)	0	0.0308	0.0014
	C_{01} (MPa)	0.1342	0	0.088
	C_{11} (MPa)	0.0889	0.027	0.011
Ogden	μ_1 (MPa)	0.00034	63.49	0.244
	μ_2 (MPa)	0.1316	0.041103	0.0146
	α_1	7.8	6.371E-10	1.018
	α_2	3.67	3.81166	3.74
	Bulk Modulus (MPa)	1,214	962	739

While the introduction of curing agents and thinner materials is an important way of controlling PDMS properties, tensile testing of the soft material is rather challenging because of a non-standard region at the beginning of the strain-strain curve. This is often caused by a misalignment between the sample and the testing apparatus when measurements have to be taken not on the sample itself, but between the grips of the tensile testing machine. This issue was

discussed by Wang, et al. while evaluating different compression and nano-indentation test methods suitable for soft materials. The authors used a specially designed compression testing machine in which the softer samples could be tested in accordance with the ASTM standards [29]. The test apparatus used by the authors is shown in Figure 13.

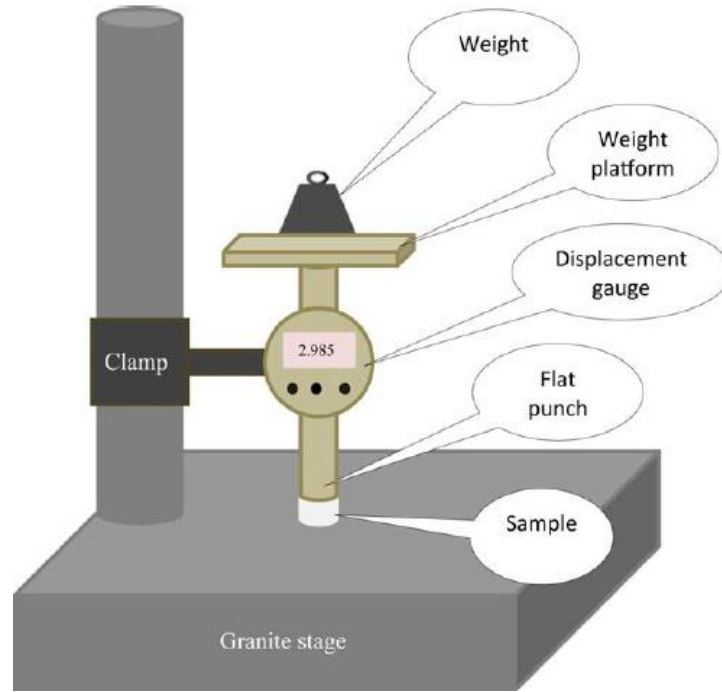


Figure 13 Custom test apparatus for determining mechanical properties of PDMS with different amount of cross-linking. Adapted from [29].

The samples were prepared by taking mixtures with varying ratios of the polymer and the curing agent, and the mixtures were poured into a flat bottomed polystyrene dish followed by degassing and curing at 65 °C. As already discussed in this literature review, it was observed that the elastic moduli of the samples decreased as polymer content increased. For example the E values of 4 mm diameter samples decreased from 3.6 MPa to 0.5 MPa as the polymer to curing agent ratio changed from 5:1 to 33:1. The rate of decrease was found to be almost linear and the authors developed an empirical relation to express elastic modulus E in terms of the PDMS to

curing agent weight ratio, n, as follows:

$$E = \frac{20\text{MPa}}{n} \quad (19)$$

The authors also found that higher amounts of the cross-linker stiffened the PDMS network, but the E value decreased thereafter as most cross-link sites became saturated and the curing agent created gaps in the network [2, 29].

2.4 Viscoelasticity Measurements Using Compression Testing

Material properties of PDMS samples have been investigated using a variety of compression and nanoindentation tests and the results have been reported in the literature. The nanoindentation technique has been found to be particularly useful for finding the elastic moduli of soft samples, especially those having low curing agent quantities with E values less than 1 MPa.

One of the early papers discussing the elastic modulus value of PDMS and other polymers found using nanoindentation was by White et al. [30]. They found that rheological properties were similar at macro and micro scales when the degree of crosslinking was greater, or the material was stiffer. However, properties were different in case of Sylgard 184 samples with an elastomer to curing agent ratio of 10:1, which made the sample more compliant [2, 29, 30].

Mechanical properties of PDMS were determined using the Maxwell model under uniaxial compression, dynamic mechanical analysis, and nanoindentation by Lin et al [31]. The authors carried out viscoelastic characterization and finite element analysis (FEA) of the three types of samples – bulk, films and micro-pillar arrays. The first two types of samples underwent punch and dynamic mechanical analysis (DMA) tests, while the arrays underwent nanoindentation to find out bending forces for individual micro-pillars. The authors obtained

loading-deformation curves in order to calculate the Young's modulus, stress-relaxation testing curves, and viscoelasticity values of the bulk and film samples using both flat punch test and Dynamic Mechanical Analysis (DMA) [31]. The complex moduli of the bulk samples were obtained using a viscoelastic FEA model and by applying a cylindrical load at different frequencies. Storage and loss moduli at different samples stiffness were obtained. Sample properties at the micro level were obtained by controlling both the deformation and reaction forces during nano-indentation. Both experimental and simulated stress-relaxation curves were plotted. Some of the results obtained by the authors are shown in Figure 14.

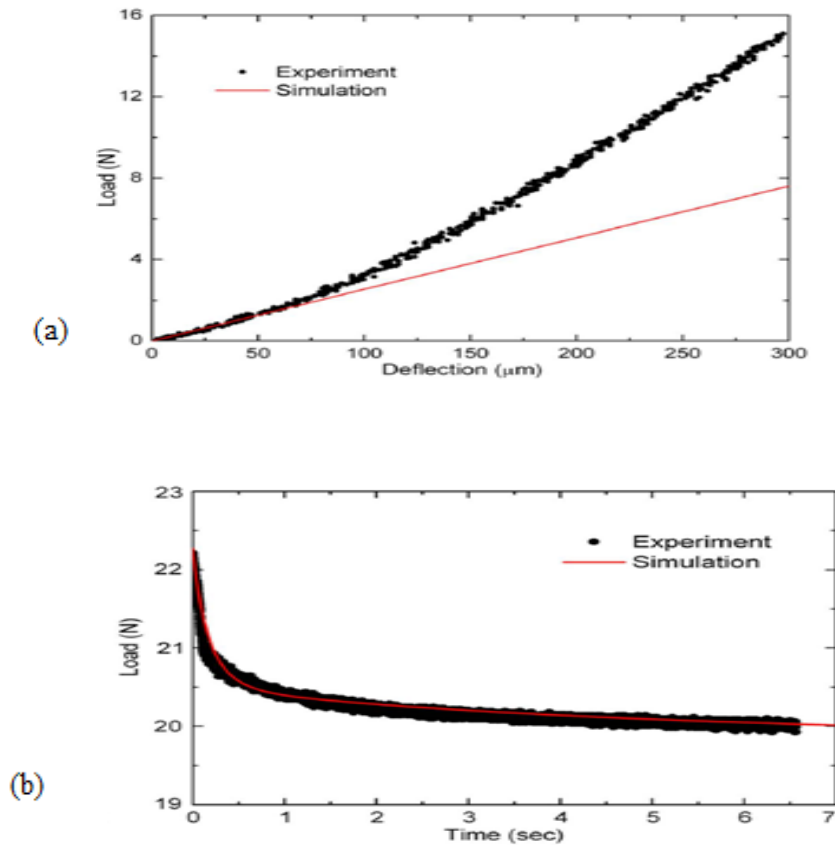


Figure 14 (a, b) Experimental and simulated curves showing load-deflection results and stress-relaxation results during punch test of PDMS samples; (c) Bulk storage and loss moduli at different loading frequencies under compression testing; and (d) Bulk stiffness values at different frequencies under cylindrical loading. Simulated and actual values almost coincide for the tests. Adapted from [31].

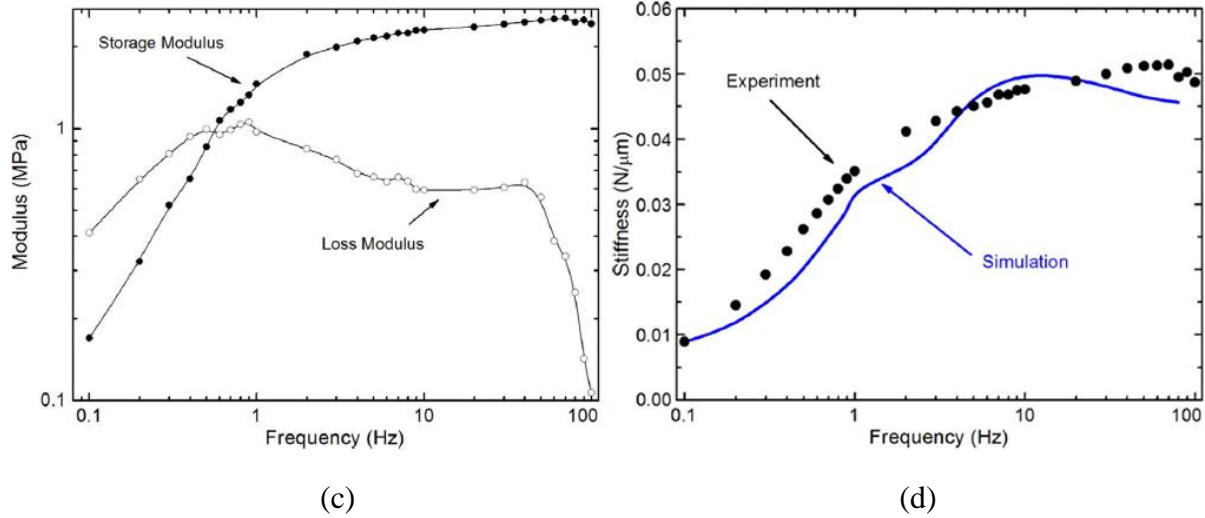


Figure 14 (Continued)

Based on results from all three tests, the authors concluded that PDMS can be best characterized as a Maxwell material, especially at the micro-pillar level, which has both elastic and viscous properties. Therefore, the behavior of the material can be adequately simulated using the Maxwell model.

Berkovich and flat punch tips were also used by Wang et al. in order to determine the elastic moduli of PDMS samples having different curing agent concentrations. They observed that the quasi-static Berkovich test has to be compensated for tip pull-in effects, and after suitable adjustments yields an E value of 1.5 MPa for a sample with a 5:1 ratio of elastomer to curing agent. They also found that the unloading stiffness value is higher, with a dynamic testing regime yielding a value of 3.6 MPa for the same sample [32].

To conclude this literature review, it can be stated that elastic modulus and other mechanical properties of PDMS depend on the extent of cross-linking (as determined by the presence of the curing agent).

CHAPTER 3: PDMS MACROSCOPIC COMPRESSION TESTING

3.1 Samples Preparation and Equipment Setup

3.1.1 Samples Preparation

The most common way to produce different base curing agent ratio PDMS is by using Sylgard 184 silicone elastomer base and Sylgard 184 silicone elastomer curing agent [2, 33-36]. Therefore, some fundamental lab materials and supplies, such as Petri dishes, spoons, cups, vacuum desiccator, gloves, weighing instrument, and hot plate are used for preparing various base curing agent ratio of polydimethylsiloxane (PDMS) samples. First of all, Sylgard 184 silicone elastomer base is placed in a cup, to determine how many grams are needed of the Sylgard 184 silicone elastomer curing agent. For instance, in the beginning of the experiment if one uses 20 g of Sylgard 184 silicone elastomer base, for making PDMS 10:1, 2 g of Sylgard 184 silicone elastomer curing agent are needed, or 4 g of the Sylgard 184 silicone elastomer curing agent are required for producing PDMS 5:1. Then, Sylgard 184 silicone elastomer curing agent is poured into the same cup and stirred until the air bubbles are not visible, and the texture becomes milky (approximately 8 to 10 minutes) [2, 33]. As shown in Figure 15, the air bubbles affect PDMS mechanical and surface properties, causing several problems with the devices, like Bio-MEMS and microfluidic devices. Hence, the goal is to minimize and remove as many bubbles as possible. Therefore, the most sustainable method to remove the bubbles is desiccator connected to a vacuum line [37].

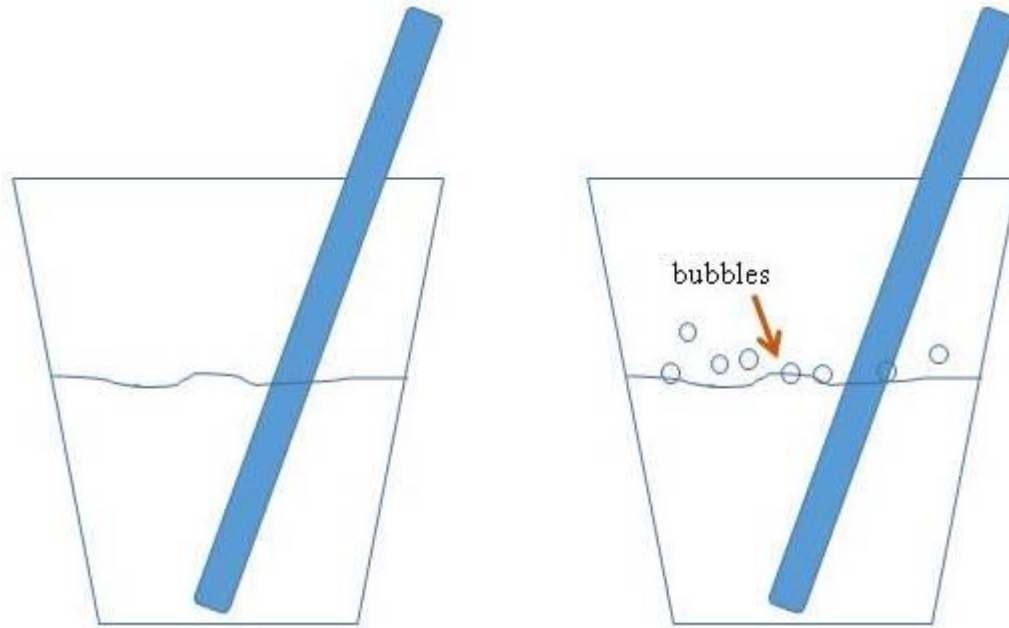


Figure 15 PDMS base is mixed with curing agent and after it is stirred, air bubbles begin to appear.

Then the polydimethylsiloxane mixture is placed in the desiccator under vacuum until no bubbles appear (about 20 to 30 min), making sure that the PDMS mixture does not foam out of the container [2, 33]. Finally, PDMS is poured over a Petri dish and placed on a hot plate at 150 °F (~65 °C), and let the polydimethylsiloxane network cure for half a day [2, 33].

According to the ASTM D1229 – 03 Standard Test Method for Rubber Property- Compression Set at Low Temperatures and ASTM Mechanical Testing and Evaluation, the aspect ratio (diameter/length) for soft materials and polymer samples should be more than 0.5 for the compression test [2, 35-37]. Punches with different diameters ($\frac{1}{8}$ ", $\frac{3}{32}$ ", and $\frac{2}{16}$ ") were used to make cylindrical polydimethylsiloxane samples. Figure 16 clearly shows the various sizes of PDMS network samples. Electronic indicator and micrometer calipers were used for measuring the length and diameter of the PDMS samples [2].

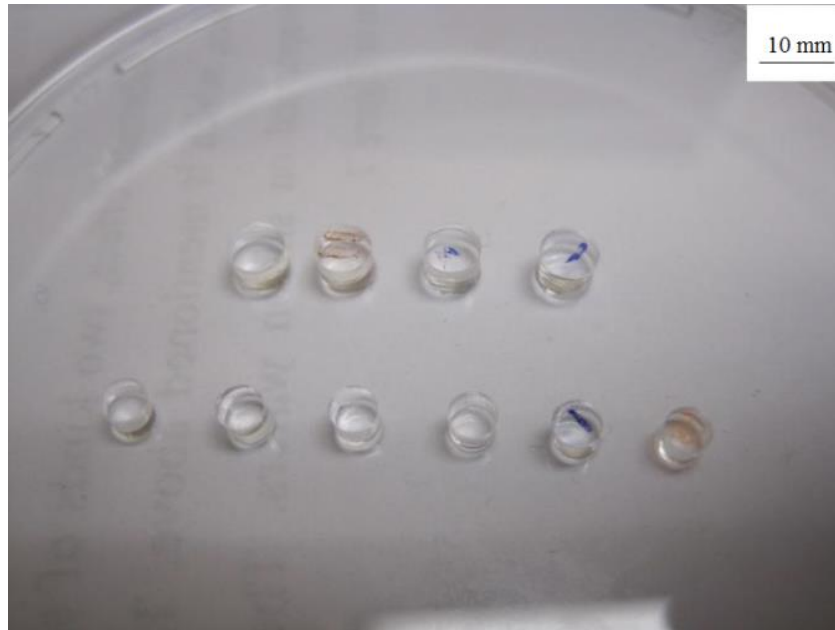


Figure 16 Cylindrical PDMS network samples for compression tests. Adapted from [2].

3.1.2 Compression Test Equipment Setup

PDMS is a soft polymeric material. Hence, simple electronic displacement indicators and displacement gauges are more suitable devices for measuring PDMS samples length changing during the compression test [2]. Mitutoyo electronic absolute digital indicator ID-C Series 543-263B and Anytime Tooling digital electronic indicator dial gauges were used in this project. Both of these digital indicators provide easy reading of the data and high accuracy. Also, they can display both inch and metric scales, with the corresponding resolution of 0.00005" and 0.001mm [39, 40].

The compression device was modified by adding digital displacement gauges to measure the lateral strain of the sample, which allowed the true stress-strain data to be obtained. Figure 17 indicates the experimental setup of the electronic gauge indicators.

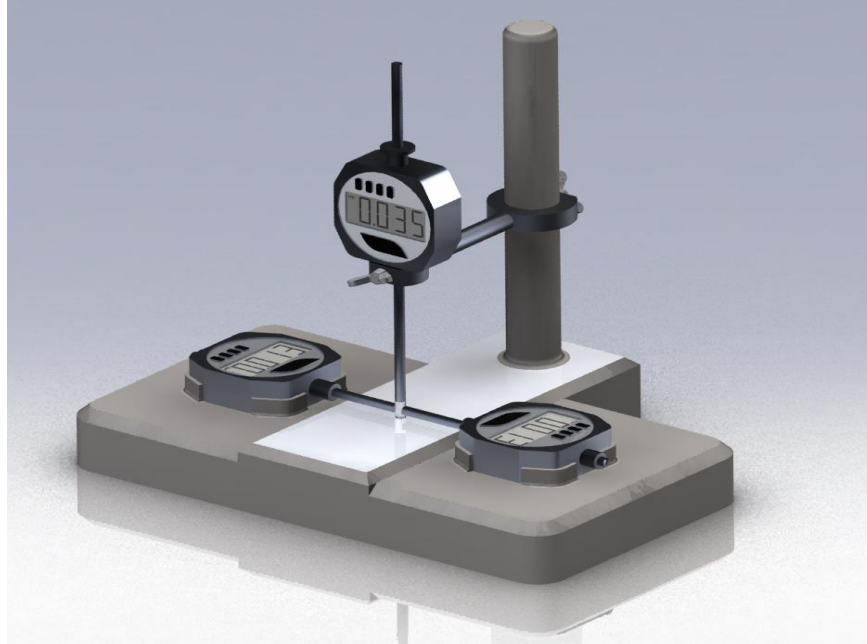


Figure 17 PDMS compression test setup.

For determining the Poisson's ratio of PDMS, different sample were tested and Table 2 lists compression test results.

Table 2 Macroscopic compression tests results for PDMS Poisson's ratio

PDMS 10:1	Poisson's Ratio
Sample 1	0.433
Sample 2	0.444
Sample 3	0.438
Sample4	0.427
Sample5	0.404
Sample6	0.382
Average	0.421

Although PDMS theoretical Poisson's ratio is about 0.5, experimental Poisson's ratio is 0.42, which proves that the samples are different form each other. As a result, the experiment shows that electronic gauges have a friction. Therefore, preloading and gravity reduce the friction of vertical electronic gauge [2]. Hence, one vertical electronic indicator gauge can be

enough to determine elastic modulus of PDMS samples. The final compression setup for measuring elastic modulus is shown in the Figure 18.



Figure 18 PDMS compression setup for measuring elastic modulus [2].

3.2 PDMS Elastic Modulus Experimental Test Results

First of all, sample diameter and length can be measured by electronic indicator or digital displacement gauge. When determining the diameter, both stress and cross-sectional areas are found. Chapter 1 mentions how elastic modulus can be found theoretically, which represents fundamental formulas for the elastic modulus. For an ideal elastic solid, the Hooke's law expresses the Young's modulus or Elastic modulus, E as:

$$E = \frac{\sigma}{\varepsilon} ; \sigma = \frac{F}{A} = \frac{mg}{\pi r^2} \text{ and } \varepsilon = \frac{\Delta l}{l} \quad (20)$$

Here, σ is the stress, ε is the strain, g is gravity $\sim 9,81 \text{ m/s}^2$, m is the loading weight, r is radius of the sample and the l is the original length of the sample. Engineering stress and strain can be determined with the compression test [2].

The sample has to be in full contact with the gauge and also without enough preload before the compression test, the elastic modulus of sample will be smaller than its true value [2]. Hence, there is a need to apply preloading, in order for the compression test to give accurate

values. As an example, let's consider PDMS 10:1 sample. Figure 19 demonstrates how preloading affects the experimental results. Elastic modulus is approximately 3 MPa and the data is linear, when doing the experiment with preloading. On the other hand, without preloading, the elastic modulus is 2 MPa and data is non-linear. Furthermore, PDMS may deform under the heavy weight loading, so one needs to determine applicable weight for preloading. Preloading may change for different samples, diameter and length. In this project, if samples' diameter is larger than 2.5 mm, the weight that needs to be applied for preloading is 50 g, if samples' diameter is smaller than 2.5 mm, it is 30 g.

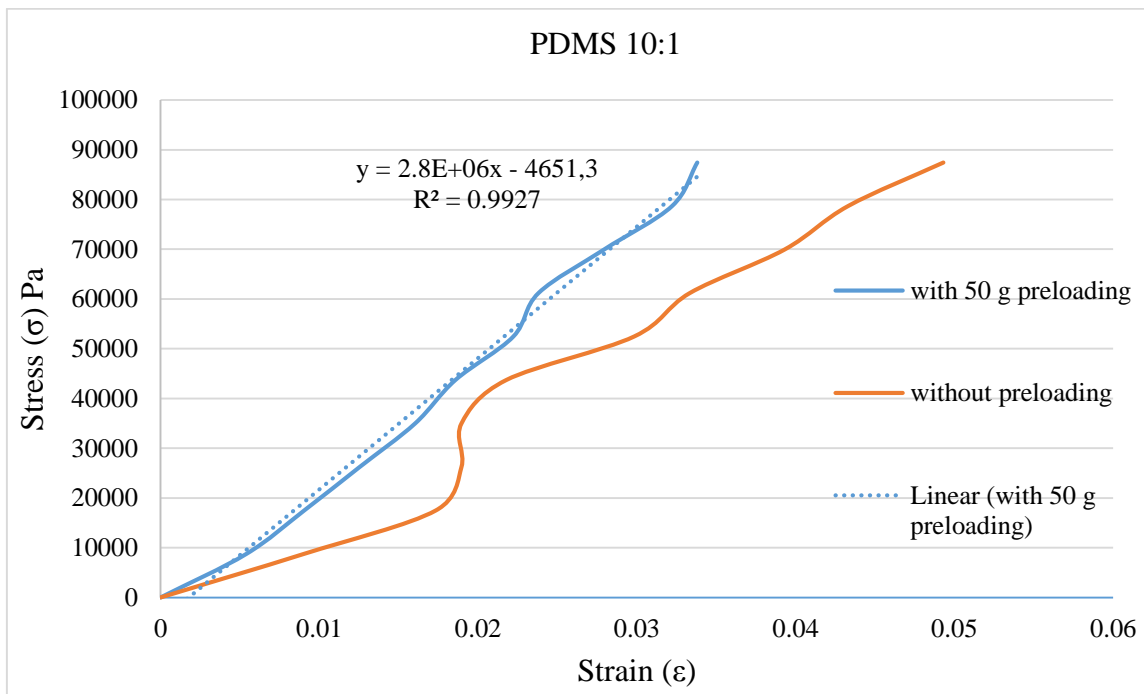


Figure 19 Comparison of preloading with no preloading on the same sample.

After the preloading is applied and the sample is fully contacted with the granite stage and the electronic gauge, the electronic gauge will be set to zero and then, the compression test will start [2].

SPSS, which is one of the most popular programs for analyzing data, and Excel were used to evaluate experimental data, such as drawing histograms, matching with normal distribution, and also finding standard derivation, mean, median, and mode of the data. The following pages demonstrate compression tests results for PDMS 5:1, PDMS 10:1, and PDMS 20:1 and their SPSS analysis results.

3.2.1 Macroscopic Test for Determining PDMS 5:1 Elastic Modulus

For determining the elastic modulus of PDMS 5:1, 48 different samples were tested and Table 3 lists compression test results.

Table 3 Macroscopic compression tests results for different samples of PDMS 5:1

Sample #	Diameter (mm)	Length (mm)	Δl	Load (g)	Area (m ²)	Force (N)	Stress, σ (MPa)	Strain (ϵ)	d/l	Elastic Modulus (MPa)
1	2.7	2.78	0.15	100	5.73E-06	0.981	0.171	0.0525	0.971223	3.262
2	2.7	3.55	0.19	100	5.73E-06	0.981	0.171	0.05352	0.760563	3.201
3	3.8	3.51	0.11	100	1.13E-05	0.981	0.0865	0.03019	1.082621	2.864
4	3.8	2.88	0.09	100	1.13E-05	0.981	0.0865	0.03125	1.319444	2.789
5	1.77	2.46	0.24	100	2.46E-06	0.981	0.398	0.0992	0.719512	4.0196
6	1.77	2	0.14	50	2.46E-06	0.4905	0.199	0.072	0.885	2.768
7	1.77	1.77	0.12	50	2.46E-06	0.4905	0.199	0.06553	1	3.0417
8	3.82	3.01	0.12	100	1.15E-05	0.981	0.0856	0.04053	1.269103	2.112
9	3.82	3.03	0.11	100	1.15E-05	0.981	0.0856	0.03762	1.260726	2.275
10	2.9	3.18	0.16	100	6.61E-06	0.981	0.149	0.04905	0.91195	3.0275
11	2.94	2.65	0.12	100	6.79E-06	0.981	0.145	0.04603	1.109434	3.1388
12	1.84	1.87	0.11	50	2.66E-06	0.4905	0.185	0.06096	0.983957	3.0258
13	1.84	2	0.12	50	2.66E-06	0.4905	0.185	0.059	0.92	3.126
14	2.86	3.13	0.13	100	6.42E-06	0.981	0.153	0.04025	0.913738	3.7933
15	2.86	2.84	0.12	100	6.42E-06	0.981	0.153	0.0436	1.007042	3.4974
16	2.8	3.16	0.13	100	6.16E-06	0.981	0.159	0.0424	0.886076	3.757
17	2.83	2.75	0.12	100	6.29E-06	0.981	0.156	0.04363	1.029091	3.574
18	1.7	2.41	0.14	50	2.27E-06	0.4905	0.216	0.05892	0.705394	3.6675
19	1.73	2.3	0.13	50	2.35E-06	0.4905	0.209	0.05826	0.752174	3.5816
20	1.84	2.43	0.13	50	2.66E-06	0.4905	0.184	0.05514	0.757202	3.3451
21	1.82	2.62	0.14	50	2.60E-06	0.4905	0.189	0.0519	0.694657	3.6322
22	1.82	1.67	0.14	50	2.60E-06	0.4905	0.189	0.08263	1.08982	2.2816
23	3.57	3.02	0.09	100	1.00E-05	0.981	0.098	0.03112	1.182119	3.14863
24	2.81	3.34	0.17	100	6.20E-06	0.981	0.158	0.05209	0.841317	3.0364
25	3.78	2.62	0.08	100	1.12E-05	0.981	0.0876	0.03206	1.442748	2.7266

Table 3 (Continued)

Sample #	Diameter (mm)	Length (mm)	Δl	Load (g)	Area (m ²)	Force (N)	Stress. σ (MPa)	Strain (ϵ)	d/l	Elastic Modulus (MPa)
26	3.8	3.36	0.09	100	1.13E-05	0.981	0.0865	0.02559	1.130952	3.3795
27	3.78	3.21	0.08	100	1.12E-05	0.981	0.08741	0.02616	1.17757	3.3405
28	3.9	2.69	0.06	100	1.19E-05	0.981	0.08212	0.02304	1.449814	3.56296
29	2.72	3.48	0.19	100	5.81E-06	0.981	0.1689	0.05402	0.781609	3.1251
30	2.82	2.7	0.17	100	6.25E-06	0.981	0.157	0.0629	1.044444	2.4946
31	2.8	3.09	0.17	100	6.16E-06	0.981	0.1591	0.05377	0.906149	2.9661
32	2.78	2.87	0.15	100	6.07E-06	0.981	0.1616	0.05226	0.968641	3.0922
33	2.8	2.94	0.22	100	6.16E-06	0.981	0.1593	0.07482	0.952381	2.1291
34	2.83	2.97	0.14	100	6.29E-06	0.981	0.156	0.04848	0.952862	3.2166
35	2.79	3.66	0.18	100	6.11E-06	0.981	0.16	0.04863	0.762295	3.2994
36	3.82	2.93	0.13	100	1.15E-05	0.981	0.0856	0.04369	1.303754	1.9593
37	3.28	3.43	0.17	100	8.45E-06	0.981	0.1161	0.04957	0.956268	2.3424
38	3.824	2.89	0.18	100	1.15E-05	0.981	0.0854	0.06159	1.323183	1.3868
39	2.91	2.33	0.12	100	6.65E-06	0.981	0.1475	0.05151	1.248927	2.86396
40	2.79	2.77	0.19	100	6.11E-06	0.981	0.1605	0.06718	1.00722	2.3896
41	2.78	2.41	0.09	50	6.07E-06	0.4905	0.08081	0.03734	1.153527	2.16388
42	1.68	3.3	0.24	50	2.22E-06	0.4905	0.221	0.07273	0.509091	3.0425
43	1.7	1.87	0.11	50	2.27E-06	0.4905	0.2161	0.0577	0.909091	3.7417
44	1.79	2.014	0.11	50	2.52E-06	0.4905	0.1949	0.05266	0.888779	3.7033
45	1.83	2.47	0.14	50	2.63E-06	0.4905	0.1865	0.05829	0.740891	3.1988
46	1.72	1.76	0.12	50	2.32E-06	0.4905	0.2111	0.06818	0.977273	3.09616
47	1.66	2.41	0.15	50	2.16E-06	0.4905	0.22665	0.06224	0.688797	3.6413
48	1.74	1.991	0.16	50	2.38E-06	0.4905	0.2063	0.08086	0.873933	2.55092

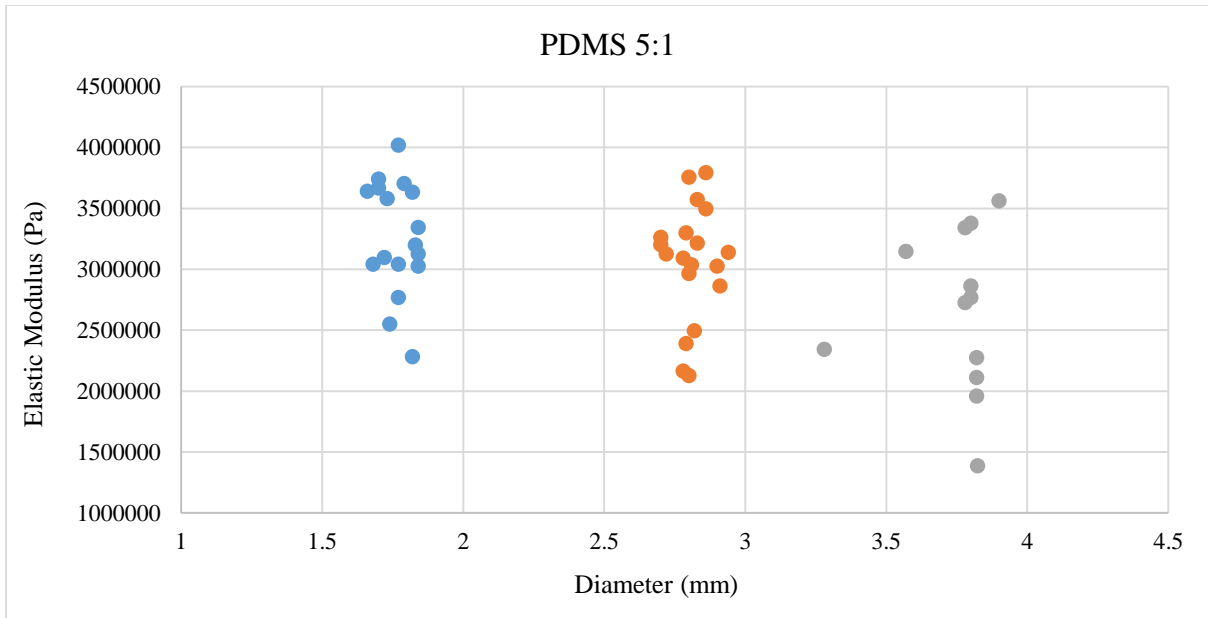


Figure 20 Distribution of different PDMS 5:1 samples' elastic modulus

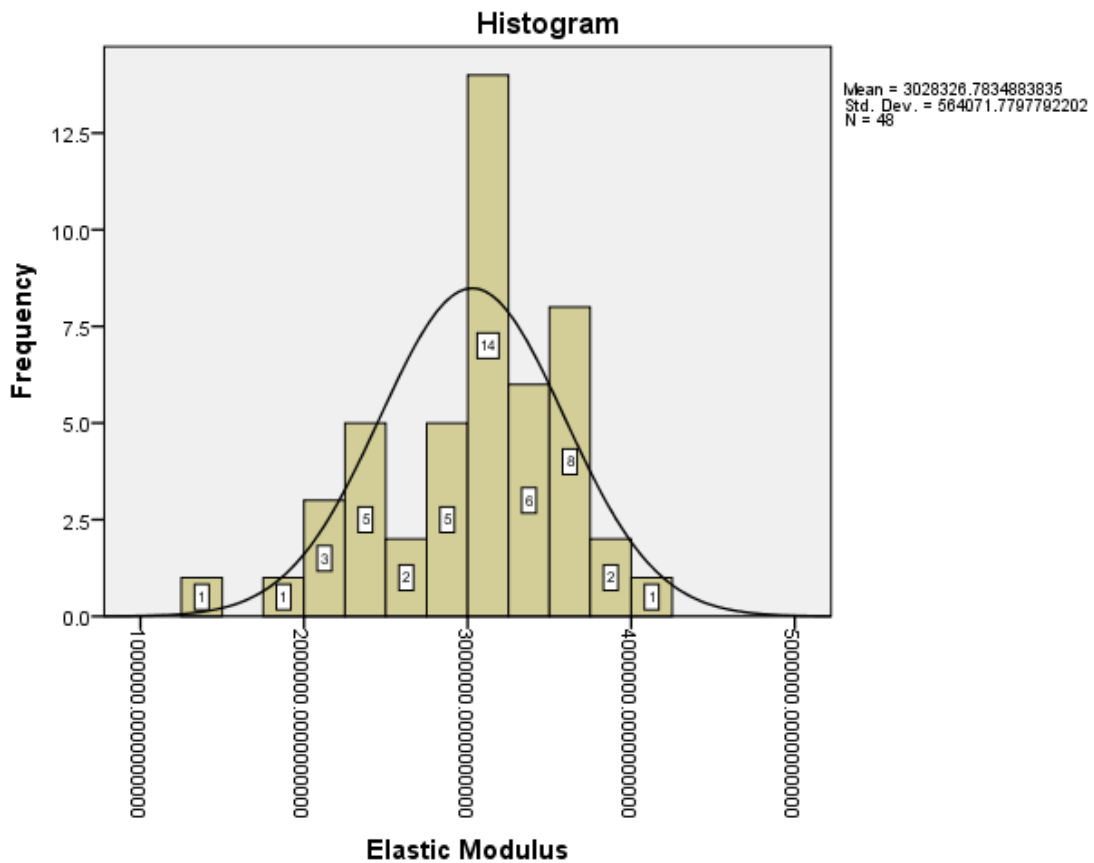


Figure 21 SPSS analyzed result of the elastic modulus of the PDMS 5:1 samples

Table 4 SPSS analyzed result of the elastic modulus of the PDMS 5:1 samples

Number of Valid Data	48.00
Number of Missing Data	0.00
Mean	3,028,326.78 Pa
Median	3,110,626.60 Pa
Mode	1386823.522 ^a Pa
Mean Standard Error	81,416.7485
Standard Deviation	564,071.78 Pa
Range	2,632,730.54 Pa
Minimum	1,386,823.52 Pa
Maximum	4,019,554.06 Pa

a. Multiple modes exist. The smallest value is shown

From Table 4 and Figure 21, elastic modulus of PDMS 5:1 is 3.03 MPa and standard derivation is 0.56 MPa. From SPSS analysis goodness-of-fit tests for normal distribution on 95% confidence interval for PDMS 5:1 histogram's the p value is 0.427, so if p value is greater than α level which is 0.05, and gives normal distribution.

3.2.2 Macroscopic Test for Determining PDMS 10:1 Elastic Modulus

For determining the elastic modulus of PDMS 10:1, 23 different samples were tested and Table 5 indicates compression test results.

Table 5 Macroscopic compression tests results for different samples of PDMS 10:1

Sample #	Diameter (mm)	Length (mm)	Δl	Load (g)	Area (m ²)	Force (N)	Stress, σ (MPa)	Strain (ϵ)	d/l	Elastic Modulus (MPa)
1	3.76	2.3	0.094	100	1.11036E-05	0.981	0.08834	0.0409	1.634782	2.1617
2	3.54	3.25	0.13	100	9.8423E-06	0.981	0.099671	0.04	1.0892309	2.4918
3	2.744	3.45	0.154	70	5.91368E-06	0.6867	0.1161	0.0446	0.795369	2.6014
4	3.62	3.36	0.102	70	1.02922E-05	0.6867	0.06672	0.0303	1.0773809	2.19786
5	3.67	2.08	0.072	70	1.05784E-05	0.6867	0.06491	0.03462	1.7644237	1.8753
6	2.76	1.876	0.066	70	5.98285E-06	0.6867	0.11478	0.03518	1.4712152	3.2625
7	2.7	3.324	0.13	70	5.72555E-06	0.6867	0.1199	0.03915	0.8122368	3.06667
8	2.82	3.01	0.138	70	6.2458E-06	0.6867	0.10994	0.04571	0.9367076	2.3981
9	2.7	2.67	0.122	70	5.72555E-06	0.6867	0.11992	0.04928	1.0135955	2.62483
10	2.79	2.77	0.114	70	6.11362E-06	0.6867	0.1123	0.04152	1.0220217	2.7293
11	2.75	2.11	0.1	70	5.93957E-06	0.6867	0.1156	0.04733	1.3317536	2.4395
12	2.8	2.75	0.196	70	6.15752E-06	0.6867	0.11153	0.07127	1.0181818	1.5647
13	2.85	2.35	0.11	70	6.3794E-06	0.6867	0.10767	0.0468	1.2165957	2.29962
14	2.82	2.69	0.106	70	6.2458E-06	0.6867	0.10997	0.0394	1.0487138	2.79014
15	2.66	2.76	0.136	70	5.55716E-06	0.6867	0.1236	0.04928	0.9637116	2.5077
16	1.75	2.71	0.186	50	2.40528E-06	0.4905	0.20394	0.0686	0.6457558	2.97115
17	1.79	2.43	0.11	50	2.51649E-06	0.4905	0.19491	0.0452	0.7366254	4.30583
18	1.73	2.21	0.104	50	2.35062E-06	0.4905	0.20864	0.04706	0.782805	4.43421
19	1.7	2.33	0.188	50	2.2698E-06	0.4905	0.2161	0.08069	0.7296134	2.67823
20	1.75	1.68	0.086	50	2.40528E-06	0.4905	0.20393	0.0512	1.0416667	3.9837
21	2.77	3.2	0.16	100	6.02628E-06	0.981	0.1628	0.05	0.8655	3.25574
22	3.55	3.33	0.1	100	9.89798E-06	0.981	0.09912	0.03003	1.0660066	3.3004
23	2.8	2.9	0.14	100	6.15752E-06	0.981	0.1593	0.0486	0.9657241	3.30015

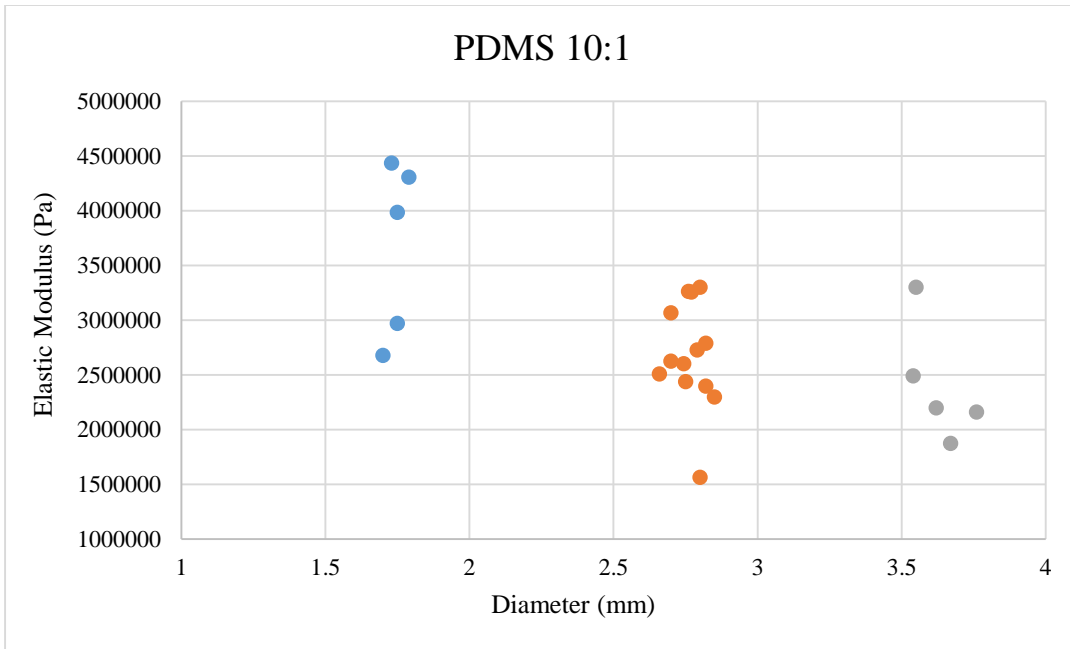


Figure 22 Distribution of different PDMS 10:1 samples' elastic modulus

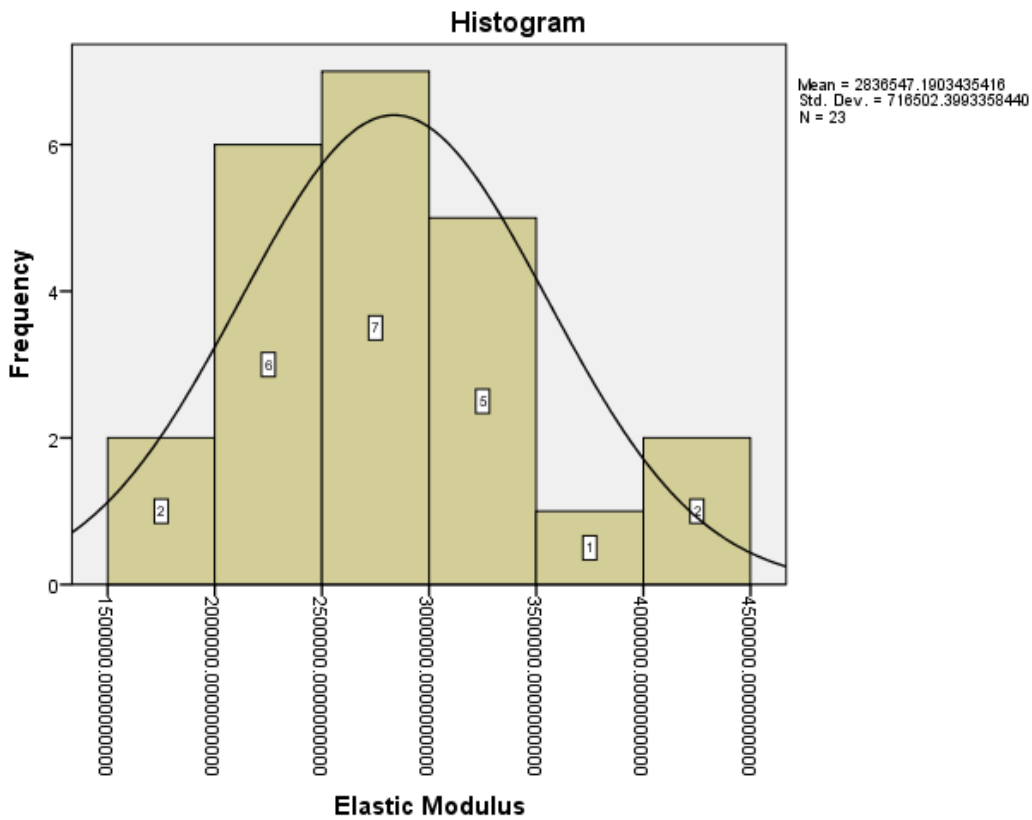


Figure 23 SPSS analyzed result of the elastic modulus of PDMS 10:1 samples

Table 6 SPSS analyzed result of the elastic modulus of PDMS 10:1 samples

Number of Valid Data	23.00
Number of Missing Data	0.00
Mean	2,836,547.19 Pa
Median	2,678,239.18 Pa
Mode	1,564,723.93486 ^a Pa
Mean Standard Error	149,401.07797 Pa
Std. Deviation	716,502.40 Pa
Range	2,869,482 Pa
Minimum	1,564,723.93 Pa
Maximum	4,434,205.93 Pa

a. Multiple modes exist. The smallest value is shown

From Table 6 and Figure 23, elastic modulus of PDMS 10:1 is 2.84 MPa and standard derivation is 0.72 MPa. From SPSS analysis goodness-of-fit tests for normal distribution on the 95% confidence interval for PDMS 10:1 histogram's the p value is 0.08, so if p value is greater than α level, which is 0.05, and gives normal distribution.

3.2.3 Macroscopic Test for Determining PDMS 20:1 Elastic Modulus

For determining the elastic modulus of PDMS 20:1, 31 different samples were tested and Table 7 clearly shows compression test results.

Table 7 Macroscopic compression tests results for different samples of PDMS 20:1

Sample #	Diameter (mm)	Length (mm)	Δl	Load (g)	Area (m ²)	Force (N)	Stress, σ (MPa)	Strain (ϵ)	d/l	Elastic Modulus (MPa)
1	3.66	3.12	0.114	50	1.05E-05	0.4905	0.04667	0.03654	1.173076	1.27549
2	3.7	2.012	0.06	50	1.08E-05	0.4905	0.045618	0.02982	1.83896	1.52976
3	3.7	2.51	0.14	50	1.08E-05	0.4905	0.045618	0.05577	1.474109	0.817886
4	3.58	2.06	0.054	50	1.01E-05	0.4905	0.048728	0.02621	1.737864	1.85894
5	3.73	3.12	0.14	50	1.09E-05	0.4905	0.044888	0.04487	1.195512	1.000362
6	3.5	2.48	0.098	50	9.62E-06	0.4905	0.050981	0.03951	1.411292	1.29014
7	2.54	1.984	0.122	50	5.07E-06	0.4905	0.096801	0.06149	1.280241	1.5742
8	2.5	1.986	0.12	50	4.91E-06	0.4905	0.099923	0.0604	1.258818	1.65374
9	1.57	1.77	0.162	30	1.94E-06	0.2943	0.15202	0.09153	0.887005	1.66096
10	1.59	1.77	0.192	30	1.99E-06	0.2943	0.148219	0.10847	0.898308	1.3664
11	1.59	1.78	0.2	30	1.99E-06	0.2943	0.148219	0.11236	0.893258	1.31916
12	3.25	3.04	0.15	50	8.30E-06	0.4905	0.05913	0.04934	1.069075	1.19822
13	3.22	2.6	0.11	50	8.14E-06	0.4905	0.06023	0.04231	1.238461	1.4237
14	2.52	1.978	0.11	50	4.99E-06	0.4905	0.098344	0.05561	1.274016	1.768401
15	2.52	1.976	0.11	50	4.99E-06	0.4905	0.098344	0.0557	1.275304	1.76661
16	1.56	1.81	0.14	30	1.91E-06	0.2943	0.15398	0.07734	0.861875	1.99068
17	1.58	1.8	0.13	20	1.96E-06	0.1962	0.100067	0.07222	0.87778	1.38555
18	2.38	1.976	0.116	50	4.45E-06	0.4905	0.110254	0.0587	1.204454	1.87818
19	2.52	1.996	0.12	50	4.99E-06	0.4905	0.098344	0.06012	1.262525	1.63572
20	1.35	2.01	0.4	50	1.43E-06	0.4905	0.342674	0.1991	0.671649	1.72194
21	1.57	1.8	0.094	20	1.94E-06	0.1962	0.101346	0.05222	0.87222	1.94068
22	2.5	1.956	0.108	50	4.91E-06	0.4905	0.099923	0.0552	1.2781761	1.80973
23	1.55	1.86	0.132	20	1.89E-06	0.1962	0.103979	0.07097	0.83333	1.46515
24	1.56	1.77	0.082	20	1.91E-06	0.1962	0.10265	0.04633	0.881356	2.21576
25	1.53	1.85	0.17	20	1.84E-06	0.1962	0.106715	0.0918919	0.82703	1.16131

Table 7 (Continued)

Sample #	Diameter (mm)	Length (mm)	Δl	Load (g)	Area (m ²)	Force (N)	Stress σ (MPa)	Strain (ϵ)	d/l	Elastic Modulus (MPa)
26	3.65	2.03	0.06	50	1.05E-05	0.4905	0.046877	0.0295567	1.79803	1.58602
27	3.65	2.04	0.06	50	1.05E-05	0.4905	0.046877	0.0294118	1.78922	1.59383
28	3.64	2.02	0.056	50	1.04E-05	0.4905	0.047135	0.0277228	1.802	1.70023
29	2.41	1.951	0.12	50	4.56E-06	0.4905	0.107526	0.0615069	1.23597	1.7482
30	1.6	1.83	0.13	20	2.01E-06	0.1962	0.097581	0.0710383	0.87694	1.37365
31	1.53	1.71	0.116	20	1.84E-06	0.1962	0.106715	0.0678363	0.894794	1.57313

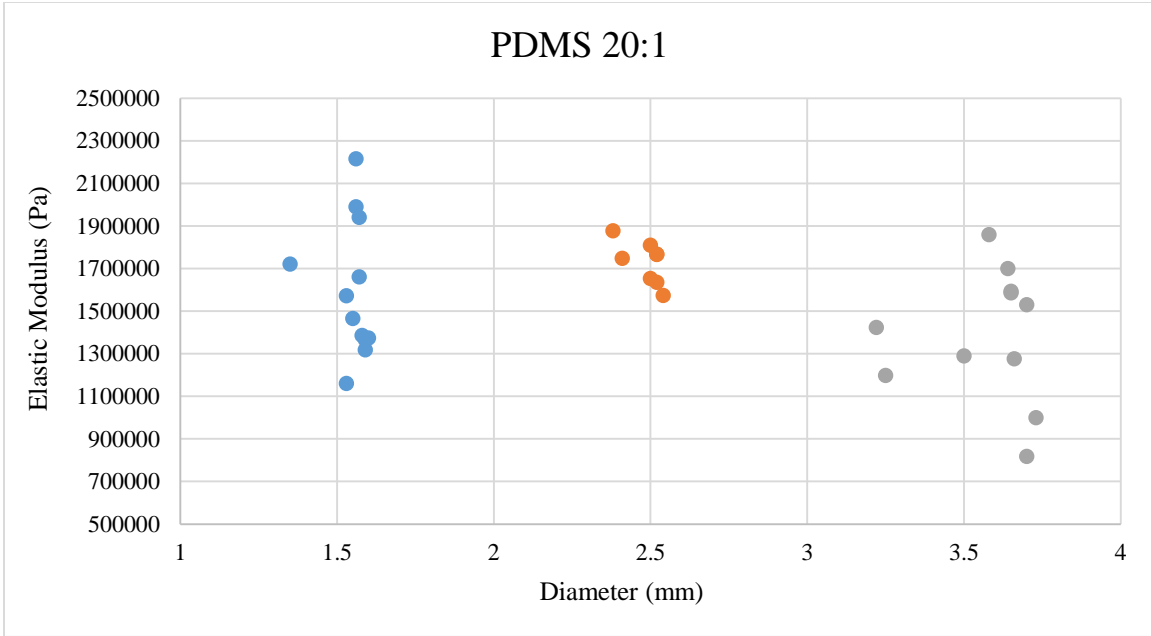


Figure 24 Distribution of different PDMS 20:1 samples' elastic modulus

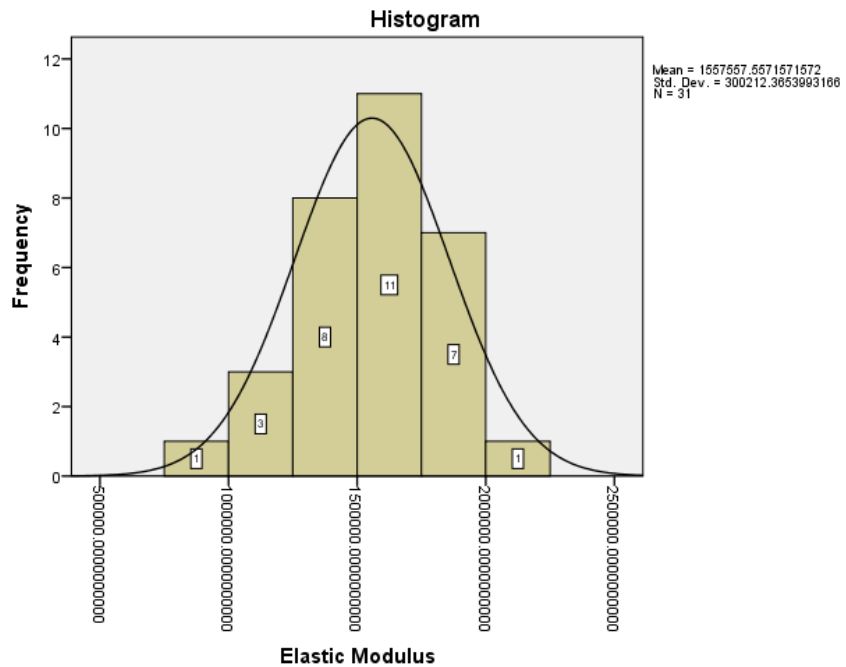


Figure 25 SPSS analyzed result of the elastic modulus of PDMS 20:1 samples

Table 8 SPSS analyzed result of the elastic modulus of PDMS 20:1 samples

Number of Valid Data	31
Number of Missing Data	0
Mean	1,557,557.56 Pa
Median	1,5860,18.28 Pa
Mode	817,883.35051 ^a Pa
Mean Standard Error	53,919.7336 Pa
Std. Deviation	300,212.37
Range	1,397,859.41 Pa
Minimum	817,883.35 Pa
Maximum	2,215,742.76 Pa

a. Multiple modes exist. The smallest value is shown

From Table 8 and Figure 25, elastic modulus of PDMS 20:1 is 1.56 MPa and standard derivation is 0.3 MPa. From the SPSS analysis goodness-of-fit tests for normal distribution on the 95% confidence interval for PDMS 20:1 the histogram's p value is 0.627, so if p value is greater than α level, which is 0.05, it gives normal distribution.

3.3 Conclusion of Macroscopic Compression Tests for PDMS Elastic Modulus

The elastic modulus results, based on the macroscopic compression tests, are indicated in the Table 9, summarizing experimental results. PDMSs' elastic modulus is connected to the samples' diameter and the base/agent ratio [2, 24, 36, 37]. Therefore, Figure 26 and Figure 30 show the relationship between the modulus of PDMS network and its base/agent ratio. The Figures 27-29 demonstrate the relationship between the modulus of PDMS samples and samples' diameter. Furthermore, Wang et al. fitting equation, which is $20/n$ and Boltzmann equation fittings are used to describe the linkage between the elastic modulus of the PDMS samples' and the relationship between the diameter and PDMS base curing agent ratio.

Table 9 Elastic modulus of PDMS sample's experimental results

	Number of Sample	Average of Diameter (mm)	Elastic Modulus (MPa)	Standard Derivation (MPa)
PDMS 5:1	12	1.7	2,66	0.47
	19	2.81	3.05	0.48
	17	3.65	3.26	0.66
Sum	48	2.68	3.03	0.56
PDMS 10:1	5	1.71	3.67	0.8
	13	2.77	2.68	0.48
	5	3.63	2.4	0.55
Sum	23	2.73	2.84	0.72
PDMS 20:1	12	1.65	1.6	0.32
	8	2.69	1.73	0.1
	11	3.57	1.39	0.31
Sum	31	2.51	1.56	0.3

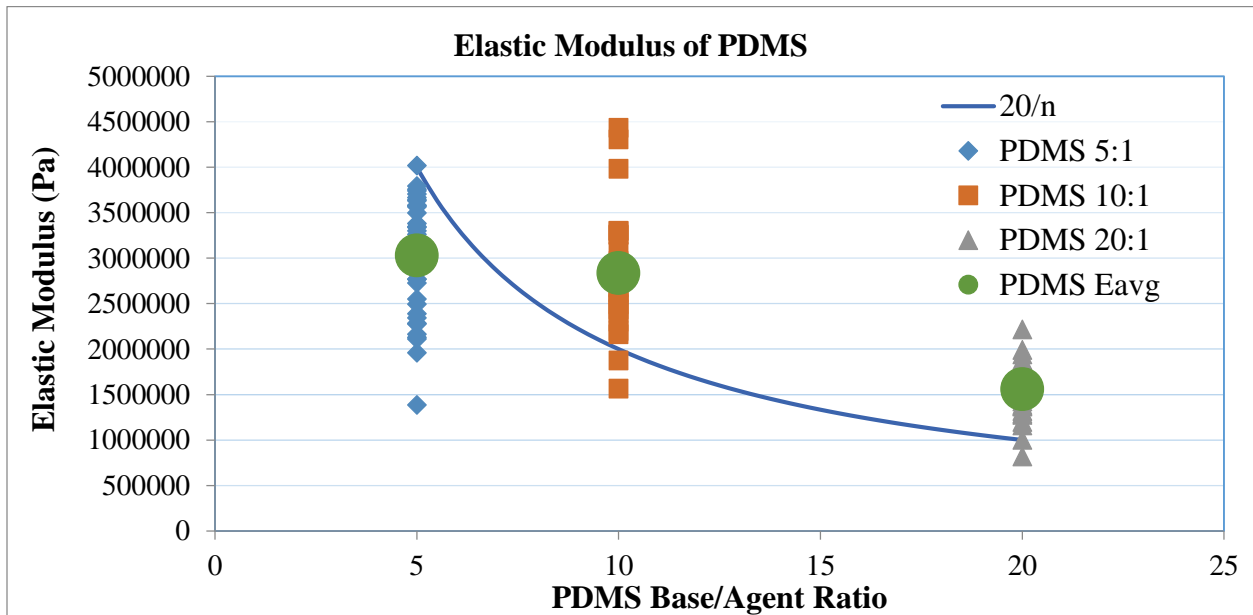


Figure 26 Distribution of different PDMS base/agent ratio samples elastic modulus

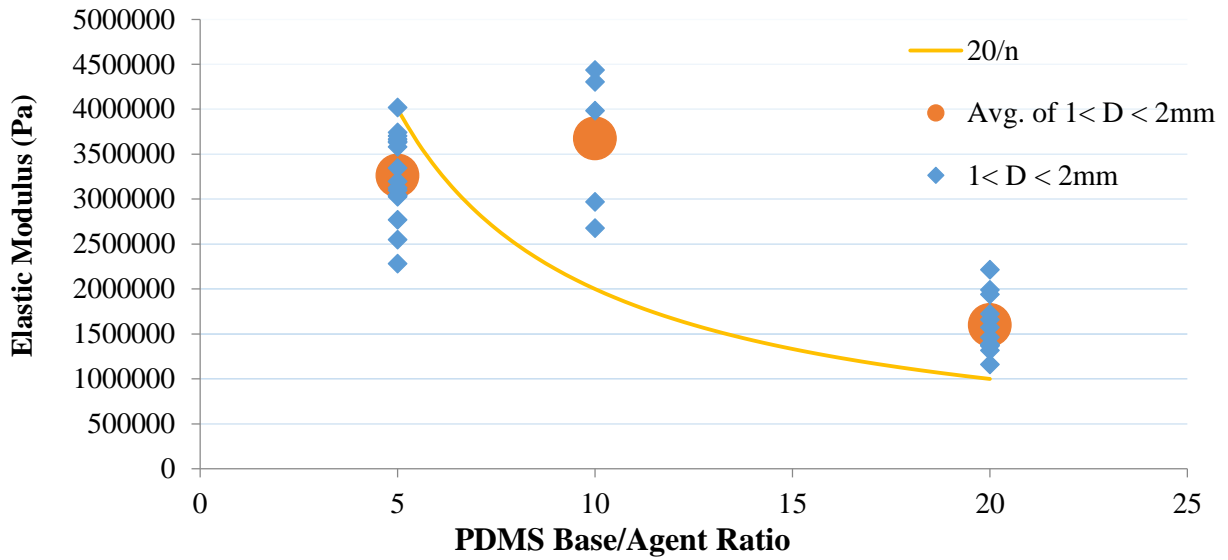


Figure 27 Distribution of diameter between 1 to 2 mm PDMS samples elastic modulus

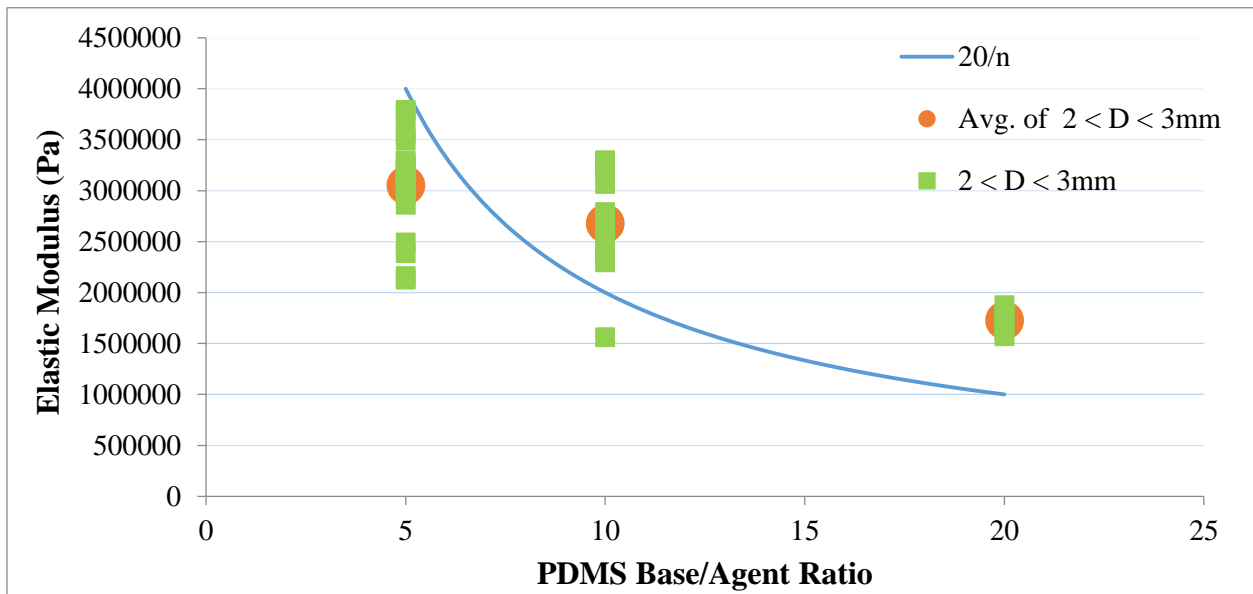


Figure 28 Distribution of diameter between 2 to 3 mm PDMS samples elastic modulus

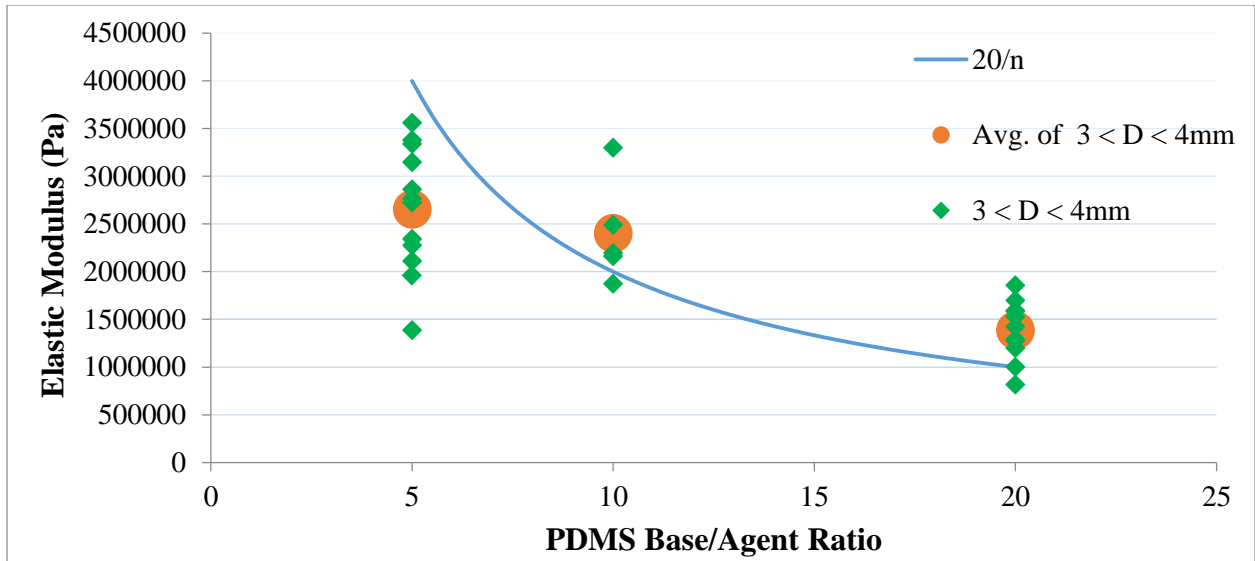


Figure 29 Distribution of diameter between 3 to 4 mm PDMS samples elastic modulus

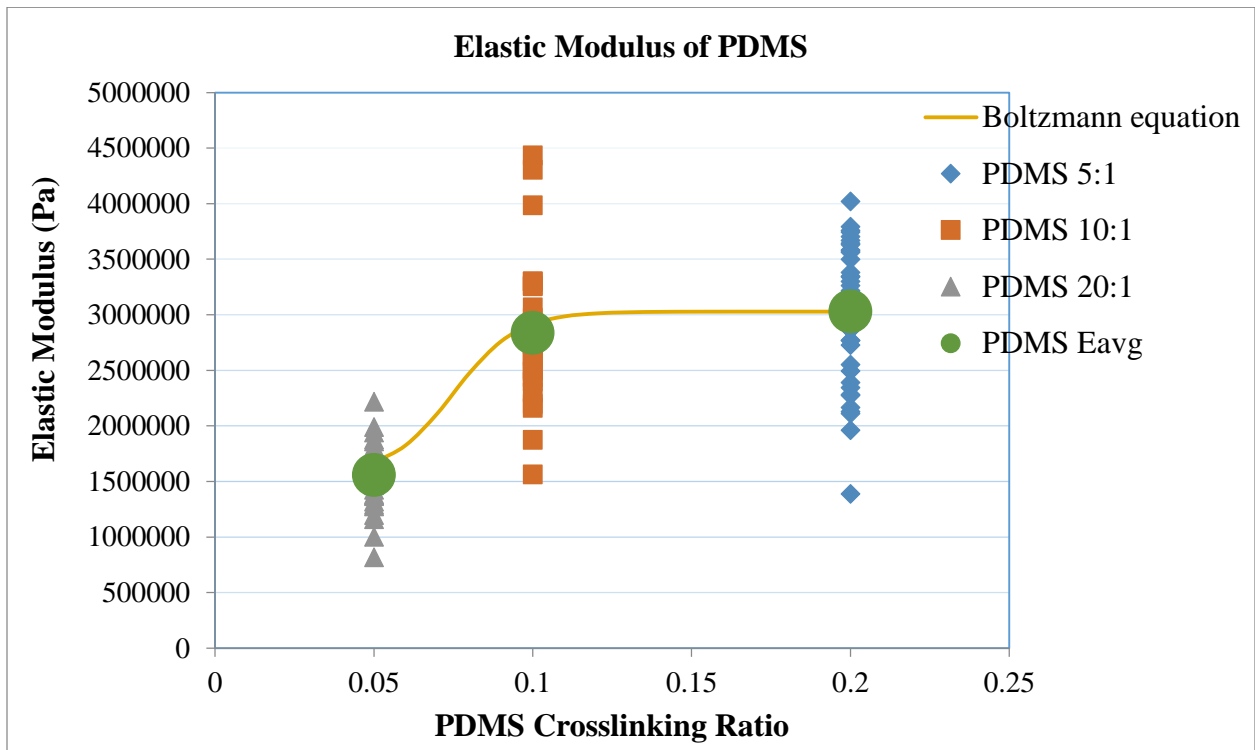


Figure 30 Distribution of different PDMS crosslinking ratio samples elastic modulus

Wang et al. in “Crosslinking Effect on Polydimethylsiloxane Elastic Modulus Measured by Custom-built Compression Instrument”, state that the elastic modulus of PDMS can be measured from the following equation:

$$E = 20/n \quad (21)$$

where n is the base curing agent ratio of PDMS [2, 29, 32]. The elastic modulus is significantly affected by samples' diameter and its base/agent ratio. In these experiments, elastic modulus varies as a result of different diameters and different base/agent ratio. Therefore, we tested a larger set of samples, which resulted in a much larger range of the measured elastic modulus. As a result, the Wang et al. fit is not adequately representing the newly collected data. Thus, an improved fit is proposed. However, softer PDMS samples with lower amount of crosslinking were not tested in this work because they are much more compliant and tacky, thus measuring of these softer samples justify a separate study. The alternative way to present the collected data is in terms of the amount of the crosslinker, or in terms of the crosslinking percentage. For this reason, the Boltzmann equation was used to fit the sigmoid curve to the data in Figure 30 plots, the same data as in Figure 26, but as a function of crosslinking.

$$E = E_0 + \frac{a}{1 + e^{\frac{N_0 - N}{b}}} \quad (22)$$

where E is the average elastic modulus in Pa of PDMS polymer at crosslinking percent of N . E_0 is the minimum value of elastic modulus in the curve. “ a ” is the maximum minus the minimum value of average elastic modulus in the curve. N_0 is the crosslinking percentage in the halfway between the highest and lowest value of elastic modulus. “ b ” is constant value related to the slope of the curve. For the data of the compression test: $a = 1,470,769$ Pa, $E_0 = 1,557,557$ Pa, $N_0 = 0.0784$, and $b = 0.012$. From SAP analyze Student's t-tests for PDMS samples distribution on

95% confidence interval for Boltzmann equation's p value is 0.84, so if p value is greater than α level which is 0.05, it is strongly similar with PDMS samples.

3.4 PDMS Viscoelasticity Experimental Test Results

The PDMS samples prepared for viscoelasticity measurements were similar to the ones described in Section 3.2. One vertical electronic indicator gauge can be enough to make simple viscoelasticity measurement for the PDMS samples. First of all, sample diameter and length can be measured by electronic indicator or digital displacement gauge. When determining the diameter, both stress and cross-sectional areas are found. Chapter 1 mentions how viscoelasticity can be found theoretically, which represents fundamental formulas and figures for viscoelasticity. In this section, two elements model (Kelvin-Voigt) and three elements model or the Zener model (standard linear solid model) were applied to PDMS samples.

3.4.1 The Kelvin–Voigt Model

Kelvin-Voigt is one of the basic viscoelasticity two element model systems. There are a spring and one dashpot in the system (Figure 31).

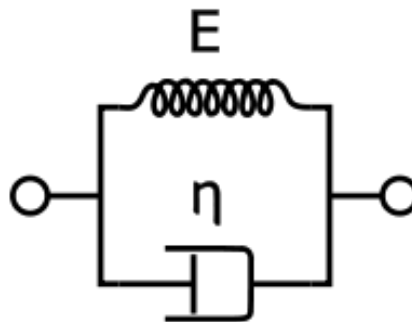


Figure 31 Schematic representation of the Kelvin–Voigt model. Released into public domain by Pekaje, 2007 [44]

In the experiment, force was applied to load the PDMS samples. In the Kelvin-Voigt model, the spring will want to stretch immediately, but is held back by the dash pot, which cannot react immediately. All the stress is thus initially taken up by the dash pot. There is no

stress in the spring because if there was there would have to be at least some strain. During the unloading part, the spring will want to contract, but again the dash pot will hold it back. However, the spring will eventually pull the dash pot back to its original zero position, given time. We expect full recovery [43]. PDMS is one of the cross-linked polymers, so the Kelvin-Voigt model can be used for the PDMS samples. Figure 32 demonstrates how strain and stress change with time under constant stress in the Kelvin-Voigt model [9, 43].

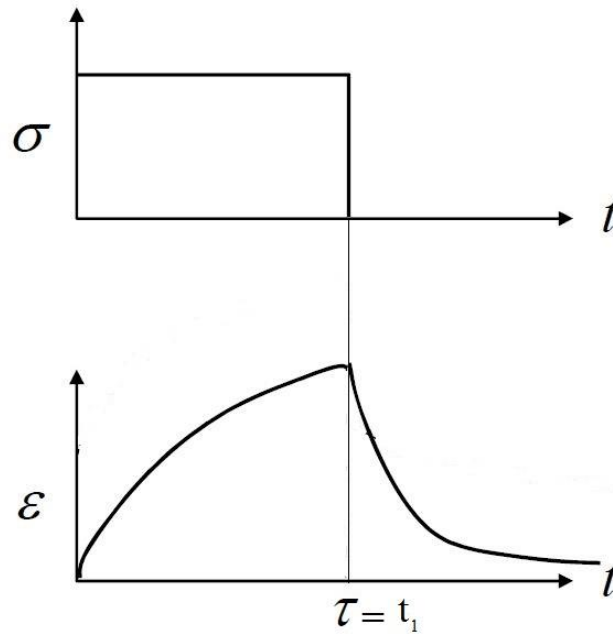


Figure 32 Applied stress and induced strain as function of time over a short period for the Kelvin-Voigt model. Adapted from [43].

The stress of a function of time can be expressed as:

$$\sigma(t) = E \varepsilon(t) + \eta \frac{d\varepsilon(t)}{dt} \quad (23)$$

$$\sigma = \frac{F}{A}; F = mg; A = \frac{\pi d^2}{4} \quad (24)$$

where E is the linear spring of the stiffness, t is the time, η is the viscosity of the dashpot, ε is the strain and also σ denotes the applied stress. F is the applied force on the material and A is the cross-sectional area of the sample. In this experiment, F does not change during the experiment and A can be accepted as a constant during the experiment [9-12, 43]. Hence, σ has a constant value.

$$\varepsilon(t) = \frac{\eta}{E} \frac{d\varepsilon(t)}{dx} - \frac{\sigma}{E} \quad (25)$$

This equation is a first order non-homogeneous ordinary differential equation and the initial condition is $\varepsilon(0) = 0$, so the equation can be solved:

$$\varepsilon(t) = \frac{\sigma}{E} \left(1 - e^{-\frac{Et}{\eta}}\right) \quad (26)$$

This experiment is comprised of the two parts, which are loading and unloading. In the loading part σ is constant with the known value. On the other hand, the unloading part of σ is zero, so the equation is separated in two parts [9, 10, 43].

For the loading part the equation is equal:

$$\varepsilon(t) = \frac{\sigma_0}{E} \left(1 - e^{-\frac{Et}{\eta}}\right) \quad (27)$$

Therefore, in the limit when (which will happen after an infinite amount of time!), the spring will carry all the stress and thus the maximum strain is $\frac{\sigma_0}{E}$, so E can be found using the experimental result [43].

$$E = \frac{\varepsilon(t_1)}{\sigma_0} \quad (28)$$

where t_1 represents the end of the loading and the beginning of the unloading time.

For the unloading ($\sigma = 0$) equation is equal:

$$\varepsilon(t) = \varepsilon(t_1) e^{-\frac{E(t-t_1)}{\eta}} \quad (29)$$

Now, t , t_1 , E and $\varepsilon(t)$ are known so, η can be easily found using the experimental output, or η can be also found with using the loading equation:

$$\lim_{t \rightarrow 0^+} \varepsilon(t) = \frac{\sigma_0}{E} \left(1 - e^{-\frac{Et}{\eta}}\right) \quad (30)$$

$$\varepsilon_1 - \varepsilon_0 = \frac{\sigma_0}{E} \left(1 - e^{-\frac{E(t-t_0)}{\eta}}\right) \quad (31)$$

Finally, all the unknowns can be found.

3.4.1.1 Comparing the Kelvin–Voigt Model with Experimental Results

For determining the viscosity of PDMS 5:1, 8 different samples were tested and Table 10 lists the compression test results.

Table 10 Macroscopic compression tests results for different samples of PDMS 5:1

	E (Pa)	η (Pa·s)	Diameter (mm)	Load (g)
1	682,944	111,952	3.78	100
2	746,347	145,987	3.7	100
3	670,990	82,743	3.68	100
4	615,414	45,184	3.64	100
5	576,159	56,013	3.66	100
6	919,335	51,693	2.58	100
7	104,3514	356,591	2.62	100
8	101,3778	230,671	2.62	100
Avg.	783,560	135,104		

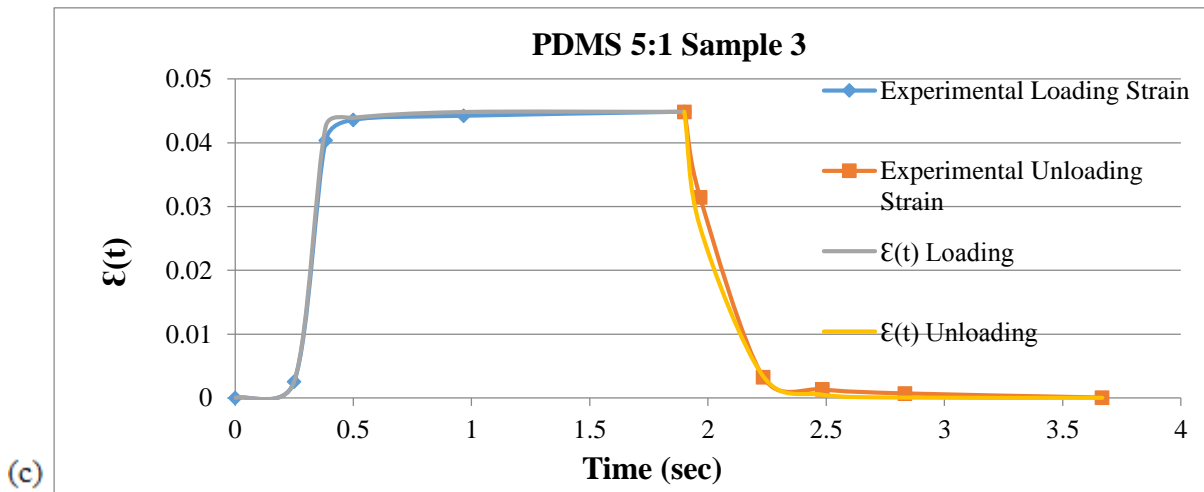
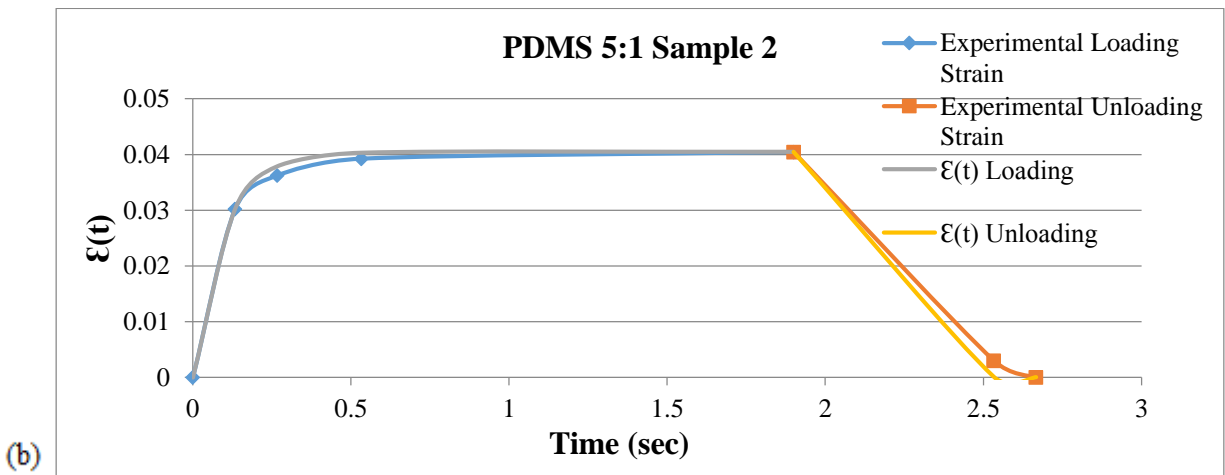
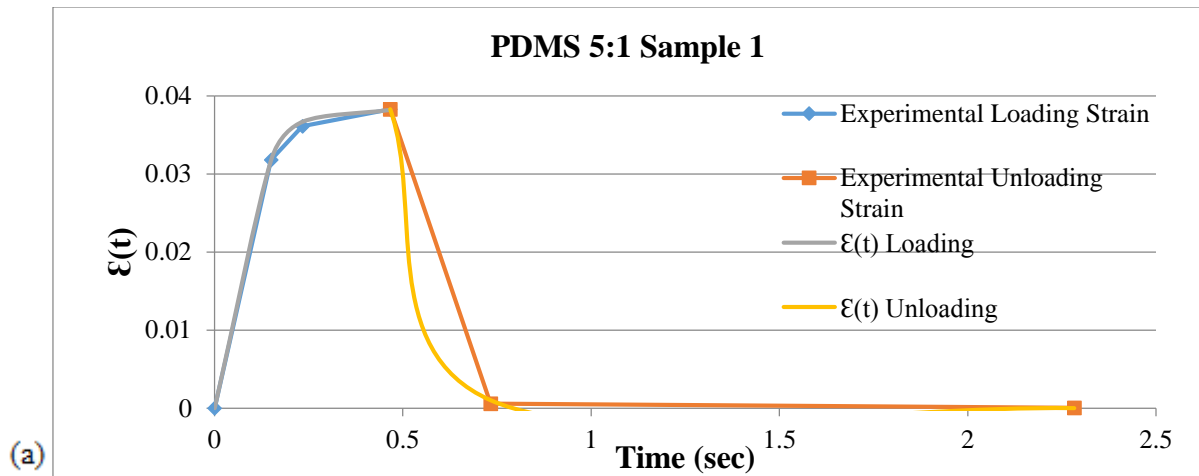


Figure 33 Comparison of PDMS 5:1 experimental results with the Kelvin - Voigt model for different samples. R^2 for these samples are (a) 0.87, (b) 0.91, and (c) 0.93

For determining the viscosity of PDMS 10:1, 10 different samples were tested and Table 11 indicates the compression test results.

Table 11 Macroscopic compression tests results for different samples of PDMS 10:1

	E (Pa)	η (Pa·s)	Diameter (mm)	Load (g)
1	686,244	60,091	3.67	100
2	553,398	75,347	3.75	100
3	553,398	75,347	3.69	100
4	521,211	132,571	3.69	100
5	604,674	32,571	3.69	100
6	584,258	134,259	3.59	100
7	584,258	134,259	2.84	100
8	767,853	134,259	2.84	100
9	767,853	134,259	2.89	100
10	874,422	134,259	2.88	100
Avg.	649,757	104,722		

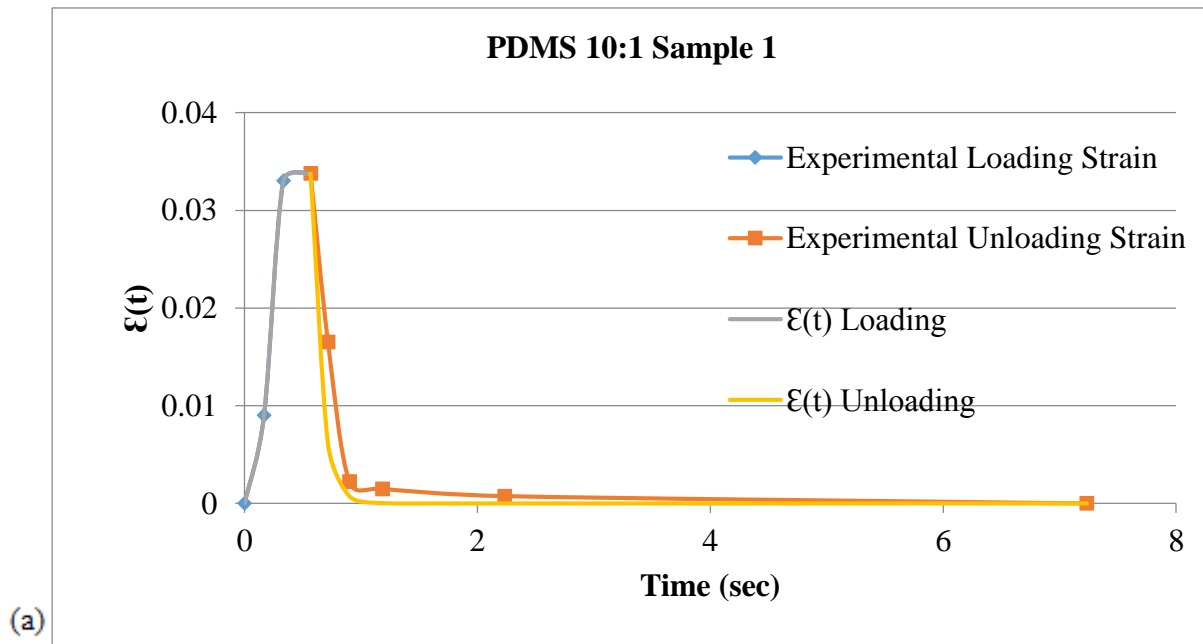


Figure 34 Comparison of PDMS 10:1 experimental results with the Kelvin - Voigt model for different samples. R^2 for these samples are (a) 0.82, (b) 0.91, and (c) 0.93

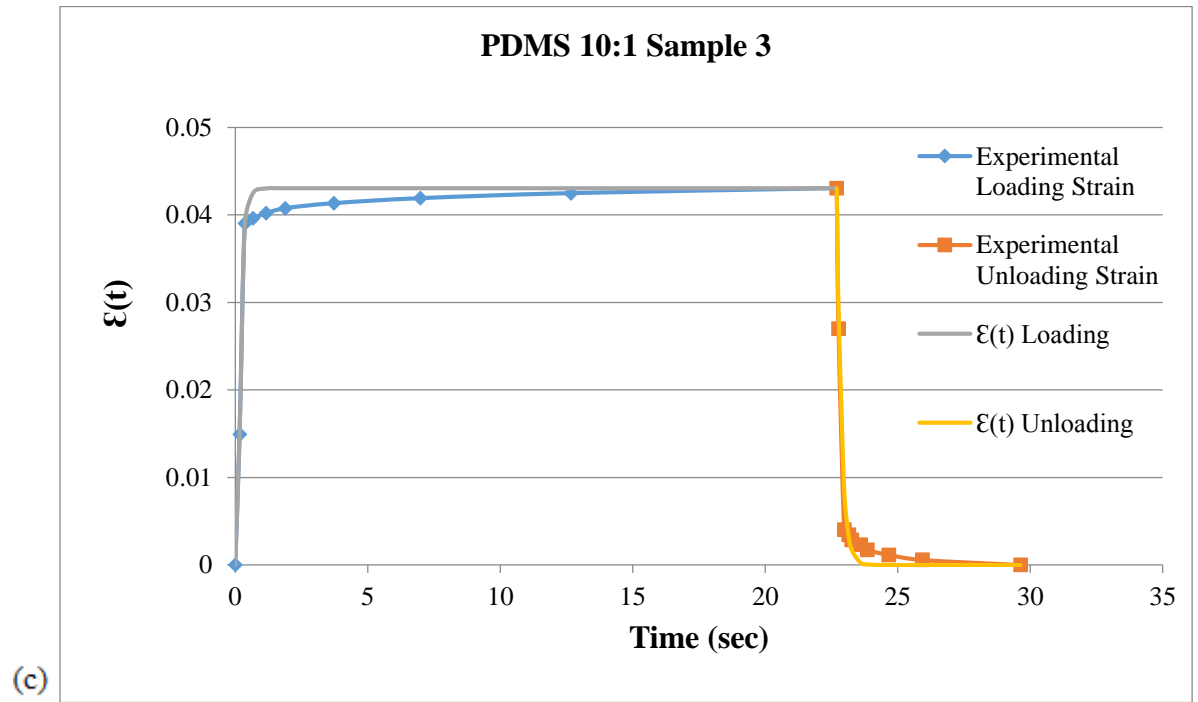
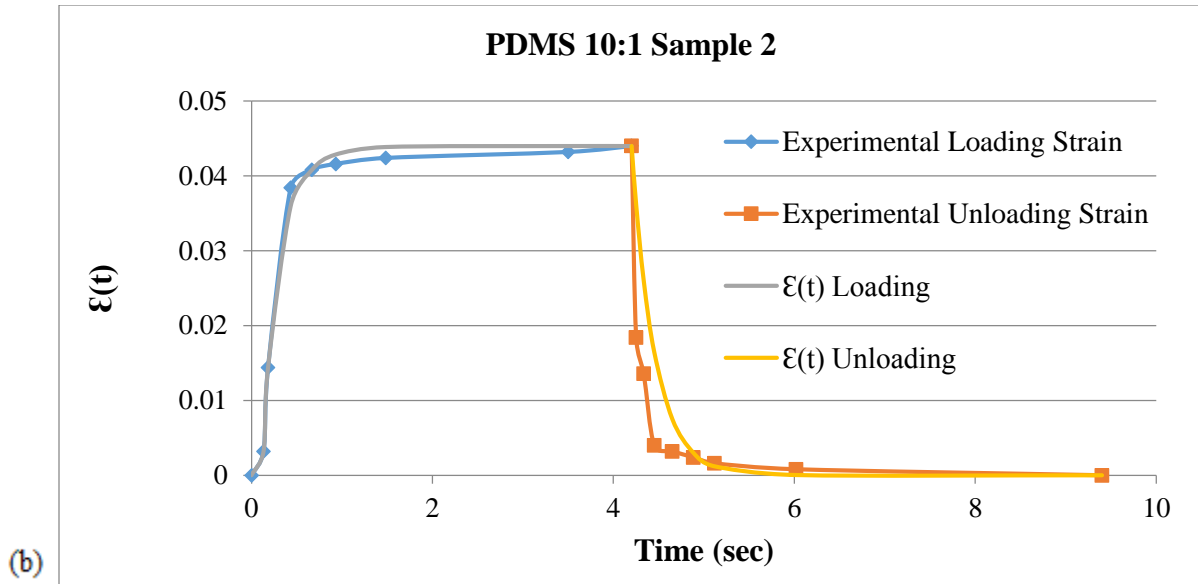


Figure 34 (Continued)

For determining the viscosity of PDMS 20:1, 10 different samples were tested and Table 12 indicates the compression test results.

Table 12 Macroscopic compression tests results for different samples of PDMS 20:1

	E (Pa)	η (Pa·s)	Diameter (mm)	Load (g)
1	563,631	71,903	3.46	50
2	543,659	71,903	3.56	50
3	513,143	71,903	3.46	50
4	513,143	71,903	3.46	50
5	436,701	70,580	3.56	50
6	436,701	70,580	3.48	50
7	403,383	75,189	3.49	50
8	541,476	110,808	3.48	50
9	638,305	71,903	2.2	50
10	770,478	71,903	1.92	50
Avg.	536,062	75,857		

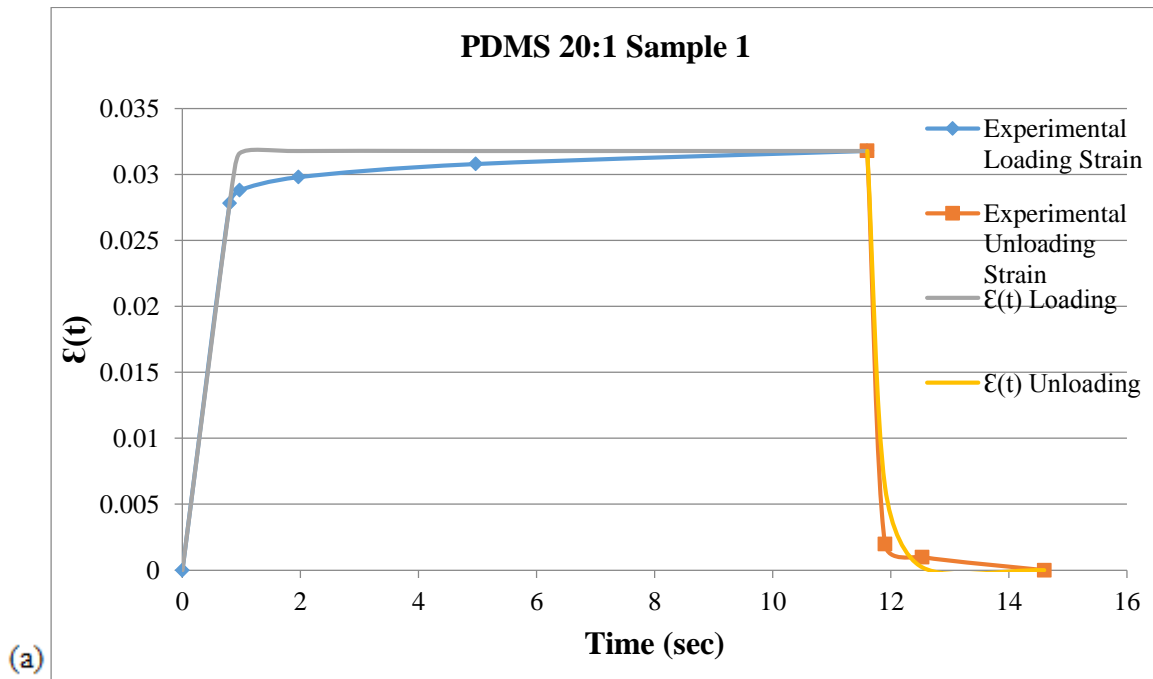


Figure 35 Comparison of PDMS 20:1 experimental results with the Kelvin - Voigt model for different samples. R^2 for these samples are (a) 0.84, (b) 0.92, and (c) 0.94

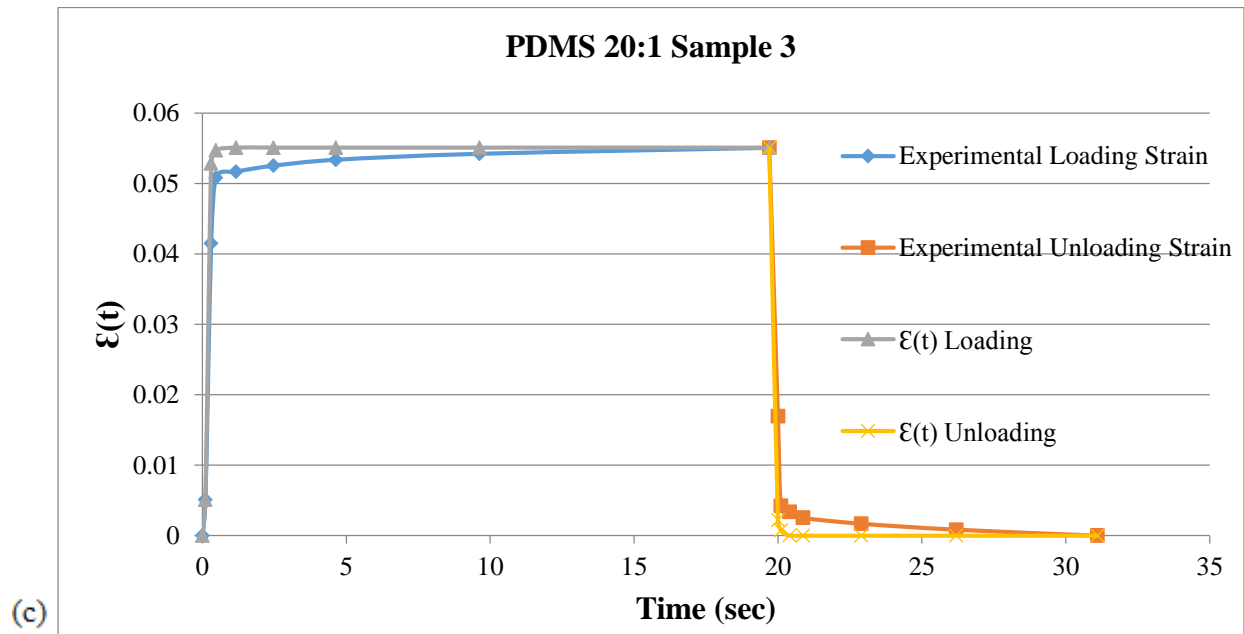
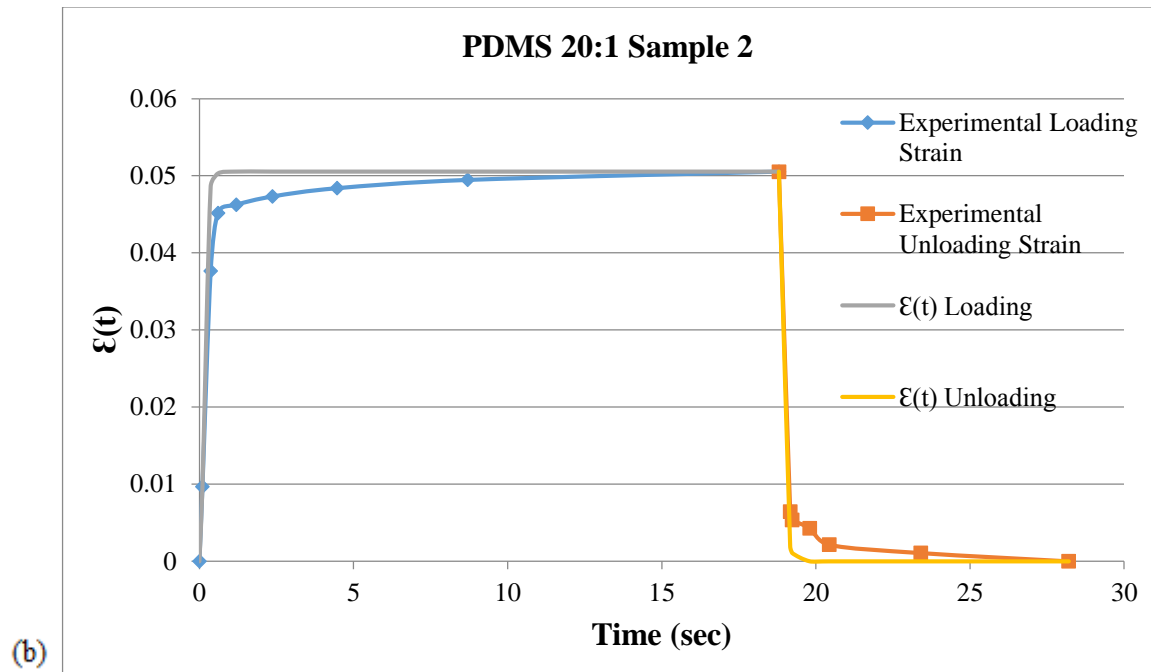


Figure 35 (Continued)

3.4.2 The Standard Linear Solid Model

The standard linear solid (SLS) model is one of the fundamental viscoelasticity three elements or the Zener model system. It is more complicated, accurate and realistic model than the Maxwell and the Kelvin-Voigt models. In contrast to the Maxwell and Kelvin-Voigt models, the SLS is slightly more complex, involving elements both in series and in parallel. Springs, which represent the elastic component of a viscoelastic material [43]. There are two springs and one dashpot in the system (Figure 36).

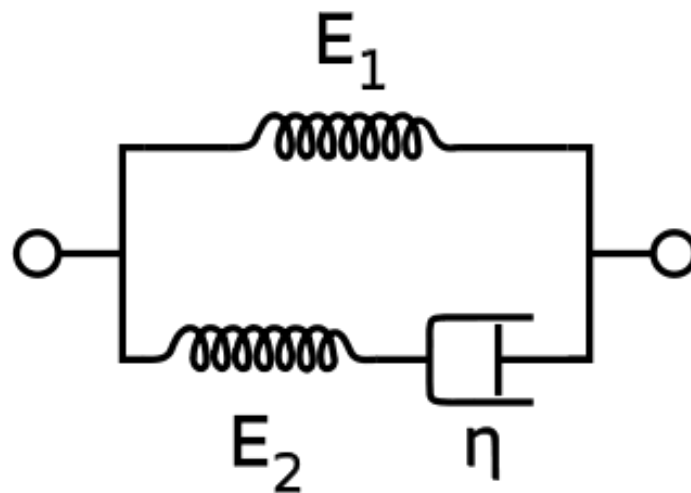


Figure 36 The standard linear solid model. Released into public domain by Pekaje, 2007 [45]

The SLS model, as expected, simplifies the recovery response of the Kelvin-Voigt unit of the model. The full response is shown in the Figure 37. This seems to be fairly close to the response of a real material, although there is no permanent strain left [43].

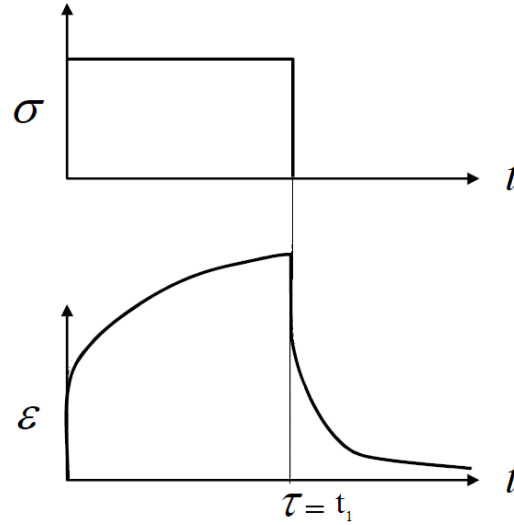


Figure 37 Applied stress and induced strain as functions of time over a short period for the SLS model. Adapted from [43].

$$\sigma + \frac{\eta}{E_2} \frac{\partial \sigma}{\partial t} = E_1 \varepsilon(t) + \frac{\eta(E_1 + E_2)}{E_2} \frac{d\varepsilon}{dt} \quad (32)$$

In this project, we can accept that the stress is applied immediately and it is constant so,

$$\frac{\partial \sigma}{\partial t} = 0$$

$$\sigma(t) = \frac{F}{A}; \quad F = mg; \quad A = \frac{\pi d^2}{4} \quad (33)$$

where E_1 and E_2 are linear springs stiffness, t is time, η is viscosity of the dashpot, ε is strain and also σ denotes applied stress, proportionality F is the applied force of the material and A is cross-sectional area of the sample. In this experiment, F does not change during the experiment and A can be accepted as constant during the experiment [9-12, 43]. Hence, σ has a constant value.

$$\sigma = E_1 \varepsilon(t) + \frac{\eta(E_1 + E_2)}{E_2} \frac{d\varepsilon}{dt} \quad (34)$$

For the loading part $\sigma \neq 0$ and σ has a constant value.

$$\lim_{t \rightarrow 0^+} \varepsilon'(t) = \frac{\sigma E_2}{\eta(E_1 + E_2)} \quad (35)$$

$$\frac{\varepsilon_1 - \varepsilon_0}{t_1 - t_0} = \frac{\sigma E_2}{\eta(E_1 + E_2)} \quad (36)$$

η can be rewritten using E_1, E_2, σ as:

$$E_1 \varepsilon(t) + \frac{\eta(E_1 + E_2)}{E_2} \frac{d\varepsilon}{dt} - \sigma = 0 \quad (37)$$

This differential equation in the form $Ax + Bx' + C = 0$. Where $A = E_1$; $B = \frac{\eta(E_1 + E_2)}{E_2}$;

$C = -\sigma$; and $x = \varepsilon(t)$. The solution to this kind of equation: $x(t) = C_1 e^{rt} + C_2 e^{-rt}$. Where

$$r = \frac{-B \pm \sqrt{B^2 - 4AC}}{2A} \text{ and, } \varepsilon(0) = 0 \text{ so, } C_1 = -C_2;$$

$$\varepsilon(t) = C_1 (e^{rt} - e^{-rt}) \quad (38)$$

C_1 represents the constant in equation 38. Therefore, in the limit on the loading part when (which will happen after an infinite amount of time!), the E_1 spring will carry all the stress and thus the maximum strain is $\frac{\sigma_0}{E_1}$, so E_1 can be found using the experimental result [43].

$$E_1 = \frac{\varepsilon(t_1)}{\sigma_0} \quad (39)$$

where t_1 represents the end of the loading and the beginning of the unloading time. Now we

don't know C_1, E_2 and η

For, the unloading ($\sigma = 0$) the equation is equal:

$$E_1 \varepsilon(t) + \frac{\eta(E_1 + E_2)}{E_2} \frac{d\varepsilon}{dt} = 0 \quad (40)$$

$$\frac{-E_1 E_2}{\eta(E_1 + E_2)} dt = \frac{\partial \varepsilon(t)}{\varepsilon(t)} \quad (41)$$

$$\varepsilon(t) = C_2 e^{\left(\frac{-E_1 E_2}{\eta(E_1 + E_2)}\right)(t - t_1)} \quad (42)$$

If $t = t_1$; $C_2 = \varepsilon(t_1)$

$$\varepsilon(t) = \varepsilon_{(t_1)} e^{\left(\frac{-E_1 E_2}{\eta(E_1 + E_2)}\right)(t - t_1)} \quad (43)$$

C_1 , E_2 and η are still unknown. Hence, if PDMS samples' viscoelastic behavior were to be modeled using the Zener model, the macroscopic compression test does not satisfy the model conditions, because more equations are needed to solve for the unknown values.

CHAPTER 4: SUMMARY AND FUTURE WORK

The main purpose of this thesis is using simple, fundamental and cheapest method for obtaining mechanical properties of soft materials. In this research, the relationship between Polydimethylsiloxane (PDMS) elastic modulus and the base/agent ratio is studied and also different viscoelasticity models are compared with experimental results.

The first chapter reviewed fundamental mechanical properties of soft material and described PDMS physical and chemical properties. The second chapter reported different scholar's research of the synthesis routes and properties of PDMS and related composite polymer materials.

Chapter three describes how most of the challenges have been overcome in this research. Reliable and sensitive macroscopic compression test equipment was created. Preloading method was applied for the macroscopic compression test to develop full contact with the sample. In sections 3.2 and 3.3, a range of PDMS samples with different base/agent ratios were tested with the macroscopic compression test. The elastic modulus of PDMS 5:1 is 3.03 MPa and its standard deviation is 0.56 MPa. The elastic modulus of PDMS 10:1 is 2.84 MPa and its standard deviation is 0.72 MPa. The elastic modulus of PDMS 20:1 is 1.56 MPa and its standard deviation is 0.3 MPa.

In this research, many samples are tested for determining to elastic modulus of PDMS. Experimental results include a large number of samples. When the same diameter (2.5 mm) and length (2.5 mm) samples are selected from two different Petri dishes, they gave totally different data. Table 13 shows compression test result for PDMS 10:1.

Table 13 PDMS 10:1 Elastic modulus on different petri dish

PDMS 10:1	Petri Dish 1 (MPa)	Petri Dish 2 (MPa)
Sample 1	2.8	3.2
Sample 2	2.7	3.7
Sample 3	3.1	2.9
Sample 4	2.6	4.5
Sample 5	2.7	2.8
Average	2.78	3.42

When the standard pen spring (221 N/m) was tested with the electronic gauge, it gave different results. Hence, it is possible that the gauge measurements are not reliable. Figure 38 and Table 14 show pen spring compression test results.

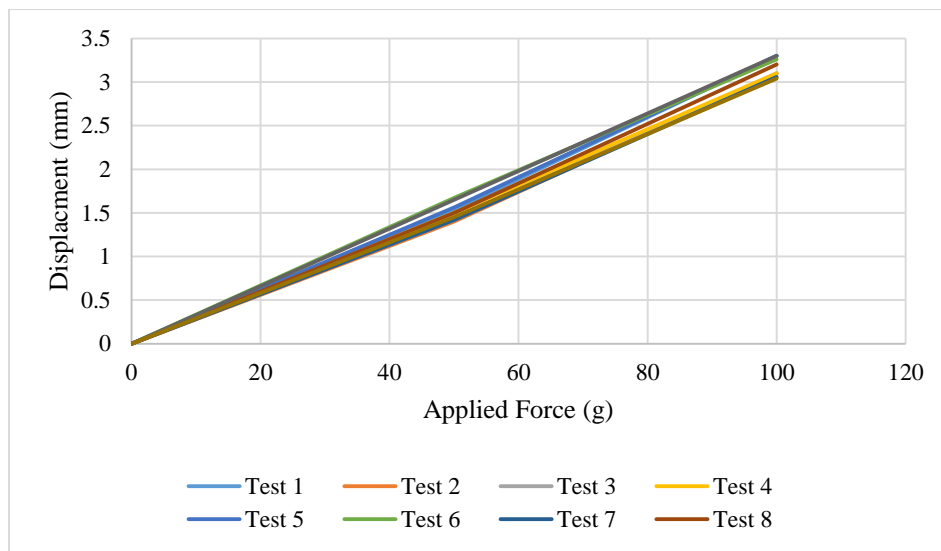


Figure 38 Standard pen spring compression test results

Table 14 Slopes of the spring compression test results

Test 1	0.033
Test 2	0.031
Test 3	0.031
Test 4	0.031
Test 5	0.033
Test 6	0.0326
Test 7	0.0306
Test 8	0.032
Test 9	0.033
Test 10	0.0304

Hence, it is shown that researcher had issues with both PDMS sample preparation and electronic displacement gauge. For the future work, researcher can prepare new samples and one can use more accurate and frictionless electronic gauge for determining the PDMS mechanical properties. Furthermore, different base/curing agent of the PDMS samples need to be tested with the compression method to obtain more accurate mechanical properties.

In the section 3.4 PDMS experimental test results are compared with the two elements viscoelasticity model. A real material does not relax with a single relaxation time. Molecular segments of varying length contribute to the relaxation, with the simpler and shorter segments relaxing much more quickly than the longer ones. This leads to a distribution of relaxation times, which in turn produces a relaxation spread over a much longer time than can be modeled accurately with a single relaxation time [9, 10]. When the researcher considers it necessary to incorporate this effect, the Zener model can have as many spring-dashpot elements as are needed to approximate the distribution satisfactorily [10]. In the future, numerical solution methods, or software programs, such as Ansys, can help to determine more accurate and realistic viscoelastic models and viscoelastic properties of PDMS.

REFERENCES

- [1] Noor, M. O., Tavares, A. J., & Krull, U. J. (2013). On-chip multiplexed solid-phase nucleic acid hybridization assay using spatial profiles of immobilized quantum dots and fluorescence resonance energy transfer. *Analytica Chimica Acta*, 788, 148-157. Retrieved January 10, 2015, from Science Direct.
- [2] Wang, Zhixin, "Polydimethylsiloxane Mechanical Properties Measured by Macroscopic Compression and Nanoindentation Techniques" (2011). *Graduate Theses and Dissertations*. <http://scholarcommons.usf.edu/etd/3402>
- [3] Bruice, P. Y. (2011). *Organic Chemistry*, 6th Ed. Illinois: Pearson, Education, Inc.
- [4] Mark, J. E.; Allcock, H. R.; West, R. "Inorganic Polymers" Prentice Hall, Englewood, NJ: 1992. ISBN 0-13-465881-7.
- [5] Teraoka, I. (2002). *Polymer Solutions an Introduction to Physical Properties*. Chichester: John Wiley & Sons. Retrieved January 11, 2015, from Wiley Online Library.
- [6] Walker, J., Halliday, D., & Resnick, R. (2014). *Fundamentals of Physics*, 10th Ed. Chichester: John Wiley & Sons, Inc. Retrieved January 15, 2015, from Wiley Online Library
- [7] Argon, A. S. (2013). *The physics of deformation and fracture of polymers*. Cambridge: Cambridge University Press.
- [8] Hosford, W. F. (2005). *Mechanical Behavior of Materials*, 2nd Ed. Cambridge: Cambridge University Press.
- [9] Basic Elasticity and Viscoelasticity. (n.d.). Retrieved February 1, 2015, from <http://press.princeton.edu/chapters/s9774.pdf>
- [10] Roylance, D. (2001). ENGINEERING VISCOELASTICITY. Retrieved February 1, 2015, from <http://web.mit.edu/course/3/3.11/www/modules/visco.pdf>
- [11] Meyers and Chawla (1999): "Mechanical Behavior of Materials," 98-103.
- [12] Dynamic Mechanical Analysis (n.d) Retrieved March 17, 2015, http://scholar.lib.vt.edu/theses/available/etd-71498-94026/unrestricted/etd_Chapt_6.pdf
- [13] Viscoelasticity (n.d) Retrieved March 17, 2015, <http://en.wikipedia.org/wiki/Viscoelasticity>

- [14] Ward, I. M. & Sweeney, J. (2004). *An Introduction to the Mechanical Properties of Solid Polymers*. Chichester: John Wiley & Sons, Inc. Retrieved January 18, 2015, from Wiley Online Library
- [15] Findley, W. N., Lai, J. S., & Onaran, K. (1989). *Creep and Relaxation of Nonlinear Viscoelastic Materials*. Amsterdam: North-Holland Publishing Company.
- [16] Rattner, B. D., Hoffman, A. S., Schoen, F. J., & Lemons, J. E. (1996). *Biomaterials Science An Introduction to Materials in Medicine*. San Diego, CA: Academic Press.
- [17] Ellis, B. & Smith, R. (2009). *Polymers: A Property Database*, 2nd Ed. Boca Raton, FL: CRC Press.
- [18] Polydimethylsiloxane. (n.d.). Retrieved January 27, 2015, from <http://en.wikipedia.org/wiki/Polydimethylsiloxane#mediaviewer/File:PmdsStructure.png>
- [19] Mark, J. E. (2007). *Physical Properties of Polymers Handbook*. New York: Springer.
- [20] Luo, T. et al. (2011). Molecular dynamics simulation of thermal energy transport in polydimethylsiloxane (PDMS). *Journal Of Applied Physics*, 109, 074321-1-6.
- [21] Owen, M J. & Dvornic, P. R. (2012). *Silicone Surface Science*. New York: Springer.
- [22] Kuo ACM (1999) *Polydimethylsiloxane*. In: Mark JE (ed) *Polymer data handbook*. OUP, New York, pp 411–435
- [23] Park, J. H., Park, K. D., & Bae, Y. H. (1999). PDMS-based polyurethanes with MPEG grafts: synthesis, characterization and platelet adhesion study. *Biomaterials*, 20, 943-953.
- [24] Hanoosh, W. S. & Abdelrazaq, E. M. (2009). Polydimethylsiloxane Toughened Epoxy Resins: Tensile Strength and Dynamic Mechanical Analysis. *Malaysian Polymer Journal*, 4(2), 52-61.
- [25] Schneider, F., Draheim, J. D., Kamberger, R. K., & Wallrabe, U. W. (2009). Process and material properties of polydimethylsiloxane (PDMS) for Optical MEMS. *Sensors and Actuators A*, 151, 95–99.
- [26] Schneider, F., Fellner, T., Wilde, J., & Wallrabe, U. W. (2008). Mechanical properties of silicones for MEMS. *J. Micromech. Microeng*, 18, 065008-065016.
- [27] Kim, T. K., Kim, J. K., & Jeong, O. C. (2011). Measurement of nonlinear mechanical properties of PDMS elastomer. *Microelectronic Engineering*, 88, 1982–1985.
- [28] Unger, M. A. et al. (2000). Monolithic micro fabricated valves and pumps by multilayer soft lithography. *Science*, 288(5463), 113-116.
- [29] Wang, Z., Volinsky, A. A., & Gallant, N. D. (2014). Crosslinking Effect on Polydimethylsiloxane Elastic Modulus Measured by Custom-Built Compression Instrument. *Journal of Applied Polymer Science*, 131(22), 41050-41053.

- [30] White, C. C. et al. (2005). Viscoelastic Characterization of Polymers Using Instrumented Indentation. II. Dynamic Testing. *Journal of Polymer Science: Part B: Polymer Physics*, 43, 1812–1824.
- [31] Lin, I-Kuan et al. (2009). Viscoelastic Characterization and Modeling of Polymer Transducers for Biological Applications. *Journal of Micro electromechanical Systems*, 18(5), 1087-1099.
- [32] Wang, Z., Volinsky, A. A., & Gallant, N. D. (2014). Nanoindentation Study of Polydimethylsiloxane Elastic Modulus Using Berkovich and Flat Punch Tips. *Journal of Applied Polymer Science*, 132(5), 41384-41390.
- [33] Molla, C. (Ed.). (2012). How to make PDMS. Retrieved February 28, 2015, from http://www.youtube.com/watch?v=zWQTnH79l_8
- [34] D.C. Duffy, J. Cooper McDonald, Olivier J.A. Schueller and G.M. Whitesides. Rapid Prototyping of Microfluidic Systems in Polydimethylsiloxane, *Anal. Chem.* 70, 1998. pp. 4974-4984.
- [35] ASM Handbook, Vol. 8, Mechanical Testing and Evaluation, ASM International, Materials Park, OH 44073-0002
- [36] Oliver WC, Pharr GM. An improved technique for determining hardness and elastic modulus using load and displacement sensing indentation experiments. *J Mater Res* (1992); 7:1564.
- [37] Microfluidics and PDMS soft lithography: PDMS degassing. (n.d.). Retrieved March 1, 2015, from <http://www.elveflow.com/soft-lithography-reviews-and-tutorials/microfluidic-device-fabrication/soft-lithography-definitions/microfluidics-and-pdms-soft-lithography-pdms-degassing>
- [38] ASTM D1229 – 03 Standard Test Method for Rubber Property-Compression Set at Low Temperatures. (2008). Retrieved March 1, 2015, from <http://www.astm.org/Standards/D1229>
- [39] Anytime Tools (2015). *1/2" DIGITAL ELECTRONIC INDICATOR DIAL GAUGE GAGE 0.00005"*. Retrieved March 1, 2015, from <http://www.anytimesale.com/1-2-DIGITAL-ELECTRONIC-INDICATOR-DIAL-GAUGE-GAGE-p/203188.htm>
- [40] Mitutoyo (2015). *ABSOLUTE Digimatic Indicator ID-C Series 543-with Max. /Min. Value Holding Function*. Retrieved March 1, 2015, from <http://ecatalog.mitutoyo.com/ABSOLUTE-Digimatic-Indicator-ID-C-Series-543-with-MaxMin-Value-Holding-Function-C1201.aspx#sthash.4VoLpbVN.dpuf>
- [41] F. Carrillo, S. Gupta, M. Balooch, S.J. Marshall, G.W. Marshall, L. Pruitt, C.M. Puttlitz. *Nanoindentation of polydimethylsiloxane elastomers: Effect of crosslinking, work of adhesion, and fluid environment on elastic modulus*. *J. Mater. Res.*, Vol. 20, No. 10, Oct 2005.

- [42] S.C. Tjong. Structural and mechanical properties of polymer nanocomposites. *Materials Science and Engineering R* 53 (2006) 73–197.
- [43] Linear Viscoelasticity Mechanical (rheological) models. (n.d.). Retrieved March 11, 2015, from http://academic.csuohio.edu/duffy_s/Linear_Visco.pdf
- [44] Kelvin–Voigt material (n.d) Retrieved March 17, 2015, from http://en.wikipedia.org/wiki/Kelvin%E2%80%93Voigt_material
- [45] Standard linear solid model (n.d) Retrieved March 17, 2015, from http://en.wikipedia.org/wiki/Standard_linear_solid_model